Pharmaceutical Research, Vol. 24, No. 3, March 2007 (© 2007)
DOI: 10.1007/s11095-006-9199-7

Featured Article

Predicting the Oxidative Metabolism of Statins: An Application of the *MetaSite*® Algorithm

Giulia Caron,[1,3] Giuseppe Ermondi,[1] and Bernard Testa[2]

Received June 5, 2006; accepted November 29, 2006; published online January 26, 2007

Purpose. This study was undertaken to examine the *MetaSite* algorithm by comparing its predictions with experimentally characterized metabolites of statins produced by cytochromes P450 (CYPs).
Methods. Seven statins were investigated, namely atorvastatin, cerivastatin, fluvastatin, pitavastatin and pravastatin which are (or were) used in their active hydroxy-acid form, and lovastatin and simvastatin which are used as the lactone prodrug. But given the fast lactone-hydroxy-acid equilibrium undergone by statins, both forms were investigated for each of the seven drugs. The *MetaSite* version 2.5.3 used here contains the homology 3D-models of CYP1A2, CYP2C19, CYP2C9, CYP2D6 and CYP3A4. In addition, we also used the crystallographic 3D-structure of human CYP2C9 and CYP3A4. To allow a better interpretation of results, the probability function $P_{SM}i$ calculated by *MetaSite* (namely the probability of atom *i* to be a site of metabolism) was explicitly decomposed into its two components, namely a recognition score *Ei* (the accessibility of atom *i*) and the chemical reactivity *Ri* of atom *i* toward oxidation reactions.
Results. The current version of *MetaSite* is known to work best with prior experimental knowledge of the cytochrome(s) P450 involved. And indeed, experimentally confirmed sites of oxidation were correctly given a high priority by *MetaSite*. In particular 77% of correct predictions (including false positive but, as discussed, this is not necessarily a shortcoming) were obtained when considering the first five metabolites indicated by MetaSite.
Conclusion. To the best of our knowledge, this is the first independent report on the software. It is expected to contribute to the development of improved versions, but above all it demonstrates that the usefulness of such softwares critically depends on human experts.

KEY WORDS: *in silico*; metabolism prediction; MetaSite; molecular fields; statins.

INTRODUCTION

Metabolism plays a major role in current drug discovery protocols, major objectives being to determine metabolic clearance, to characterize the nature, level and properties (pharmacokinetic, pharmacological and toxicological) of metabolites, and to estimate the potential for drug–drug interactions (in particular enzyme inhibition and induction). Whereas *in vitro* and *in vivo* experiments remain indispensable, there is an increasing demand for *in silico* metabolic predictions to contribute to rational drug design, help bioanalysts and biochemists, and alert toxicologists, among other objectives. From a general and schematic viewpoint, available *in silico* methods can be divided into two classes, namely specific ("local") and comprehensive ("global") ones (1,2). Comprehensive expert systems aim at offering a full view of the metabolism of a given compound. Existing databases (i.e., knowledge-based systems) can be searched to retrieve information on the known metabolism of compounds with similar structures or containing specific moieties (3,4). Predictive expert systems attempt to portray the metabolites of a compound based on knowledge rules, defining the most likely products. They recognize target groups and their metabolic reactions, and attempt to prioritize such reactions. Existing rule-based expert systems of this type are *MetabolExpert*™, (http://www.compudrug. com) *META*™ (http://www.multicase.com) and *METEOR*™ (http:// www.lhasalimited.org)(5–6).

Specific systems generally apply to specific enzymes or to specific metabolic reactions. Such systems include quantitative structure–metabolism relationships (QSMR's) based on structural, physicochemical and/or quantum mechanical properties (7,8). Various structural and physicochemical properties can be used as independent variables in such regressions, e.g., steric, electronic and/or lipophilicity parameters. Statistical methods used to search for correlations include multiple linear regression analysis, multivariate analyses, and unsupervised machine-learning approaches (neural networks and genetic algorithms) (9,10). Quantum mechanical calculations may also shed light on SMR's, revealing correlations between rates of metabolic oxidation and energy barriers in electron abstraction or homolytic C−H cleavage (11–14). Three-

Electronic supplementary material The online version of this article (doi: 10.1007/s11095-006-9199-7) contains supplementary material, which is available to authorized users.

[1] Dipartimento di Scienza e Tecnologia del Farmaco, via Giuria 9, 10125 Torino, Italy.
[2] Pharmacy Department, University Hospital, Rue du Bugnon, CH-1011 Lausanne-CHUV, Switzerland.
[3] To whom correspondence should be addressed. (e-mail: giulia.caron@unito.it)

dimensional QSMR's (3D-QSMR's) methods (e.g., Comparative Molecular Field Analysis, *CoMFA*) yield a partial view of the binding/catalytic site of a given enzyme as derived from the 3D molecular fields of a series of substrates or inhibitors (the training set) (15–17). 3D-QSMR tools yield "pharmacophores," namely a 3D-representation of the stereoelectronic features a compound must display for affinity and catalysis or inhibition. Such pharmacophores yield an indirect view of the binding/catalytic sites, and may allow a quantitative prediction for novel compounds structurally related to the training set. A recent and relevant development is based on flexible molecular interaction fields (*GRID*) and their description using alignment-independent descriptors in *ALMOND* (18,19).

As for the homology modeling of xenobiotic-metabolizing enzymes, this was made possible by the X-ray structural determination of phylogenetically related proteins. Given their assumptions, there is an inherent error in the quantitative predictions such pharmacophoric models afford. Nevertheless, outcomes with a strong affinity component (e.g., K_m, K_i and IC_{50} values) are generally well predicted. The pharmacophoric models of a large number of mammalian and mostly human CYPs are now available, as well as other xenobiotic-metabolizing enzymes such as DT-diaphorase and glutathione S-transferases (20–24). The crystallization and X-ray structural elucidation of mammalian (including human) cytochromes P450 with and without bound ligands (25,26) is a breakthrough which may refine assumptions inherent in homology modeling and will thus improve the predictive power of molecular modeling.

Note that specific systems are in principle applicable to any chemical system. However, each model handles only one metabolic reaction or catalytic mechanism at a time. Combining several specific models to form a meta-model is a most appealing if ambitious strategy and much work remains before such approaches can be seen as genuinely comprehensive. Nevertheless, the recent release of *MetaDrug*™ (http://www.geneco.com) (27) is a significant and promising step in this direction.

The HMG-CoA reductase inhibitors known as statins are a major therapeutic class of considerable value in reducing the risk of coronary events in both primary and secondary prevention (28,29). Two of the marketed statins are used in the lactone, prodrug form (e.g., lovastatin and simvastatin), while most others are used as the active hydroxy-acids (e.g., atorvastatin, fluvastatin and pravastatin) (30,31).

The metabolism of statins is a complex one. There is a non-enzymatic lactone/hydroxy-acid equilibrium which is comparatively fast under gastric conditions of acidity ($t_{1/2}$ of about 1 h with an equilibrium constant close to one) but much slower at neutral pH (30,32). Enzymatic lactone opening can also occur, in particular by serum paraoxonase (33). The carboxy group in the hydroxy-acid form of statins is an active target of phase II metabolism involving conjugates as intermediates and/or metabolites. Thus, glucuronidation of the carboxy group leads to an acyl-glucuronide which was detected in the *in vitro* metabolism of simvastatin-acid and atorvastatin, among other (5,34). These acyl-glucuronides were characterized both as metabolites and as intermediates, since they spontaneously underwent cyclization-elimination to form the δ-lactone. Another pathway is conjugation with Coenzyme A (CoA) to form a thioester. This CoA conjugate is not detectable as a stable metabolite, but is a metabolic intermediate in the β-oxidation of the hydroxy-acid side-chain as well as in its lactonization by cyclization-elimination. (35) Glucuronida-

Table I. Overview of Predictions for CYP2C9 and 3A4

Compound	Metabolite [a]	Atom [b]	CYP [c]	Position P_{SM} [d]	Position P_{SM}* [e]
Atorvastatin	*M1*	H8	3A4	9	5
	M1	H16	3A4	9	5
	M2	H12	3A4	1	1
Cerivastatin	*M1*	H30–H32	3A4	1	1
	(*M2*)	(H17–H19)	(2C8)	(3)[f]	–
Fluvastatin	*M1*	H52	2C9	1	2
	M2	H54	2C9	3	4
	M3	H40	2C9	2	1
Lovastatin	*M1, M2*	H44	3A4	1	1
	M3	H54–H56	3A4	2	3
Pitavastatin	*M1*	H4	3A4	5	7
	M2	H39	2C9	1	1
Pravastatin	*M1*	H59	3A4	5	13
	M2	H48	3A4	22	7
Simvastatin	*M1*	H44	3A4	1	1
	M1	H44	2C9	1	1
	M2	H54–H56	3A4	2	3
	M2	H54–H56	2C9	2	3
	M3	H54–H56	3A4	2	3
	M3	H54–H56	3A4	2	3
	M4	H47	3A4?	24	13

[a] Experimentally observed metabolite, see corresponding Figure for structure.
[b] Atom(s) indicating the site of metabolism.
[c] CYP isoenzyme involved in the formation of the metabolite (see also corresponding Figure).
[d] Rank of site of metabolic attack by the corresponding CYP enzyme, as predicted by *MetaSite* using its built-in homology model.
[e] Rank of site of metabolic attack by the corresponding CYP enzyme, as predicted by *MetaSite* using an imported crystallographic structure.
[f] CYP2C9 prediction.

tion and sulfation of hydroxy groups elsewhere in the molecules are also known. But the major metabolic reactions are catalyzed by cytochromes P450 and involve oxidation of aliphatic carbons, alkenyl groups and aromatic rings. Subsequent reactions include N-dealkylations, dehydration to form $C = C$ double bonds, dehydrogenation of primary alcohols to an aldehyde and then a carboxylic acid, and glutathione conjugation of epoxides (33,34,36,37).

Given the huge medical significance of statins, their complex molecular structure and the major role played by cytochromes P450 (CYPs) in their metabolism, we reasoned that these drugs could provide a clinically relevant challenge to a software simulating human CYP-mediated oxidation. *MetaSite*® is one of the most recent and well-published CYP-specific algorithm currently available, and it was chosen in this study to compare experimental data with its predictions (retrodiction would be the correct term here). Rather than examining the predictions of many substrates and reporting statistics of correct and false positive (18,38), our objective here was an in depth analysis of the prediction of a few structurally complex substrates with a view to contribute constructively to the further improvement of the algorithm. In fact the information gained from a huge series of heterogeneous compounds can be very different from the one obtained from a small series of correlated drugs but both approaches are necessary for a better assessment of the benefits and limits of such a complex computational tool.

THEORETICAL BACKGROUND

MetaSite is a specific system in the sense that it is currently restricted to the major human cytochromes P450 (i.e., CYPs), and more specifically to CYP-mediated carbon oxidation (18,19,38–40). Reactions of reduction generally remain to be implemented. The methodology of *MetaSite* is based on a combination of QSAR's and molecular modeling and involves the calculation of one set of descriptor set for the enzyme protein (built by homology model as implemented in the actual version of the software) and another set of descriptors for each substrate. Both sets of descriptors are based on Molecular Interaction Fields (MIF's) generated by GRID (41–44). At the end of the procedure the two sets are

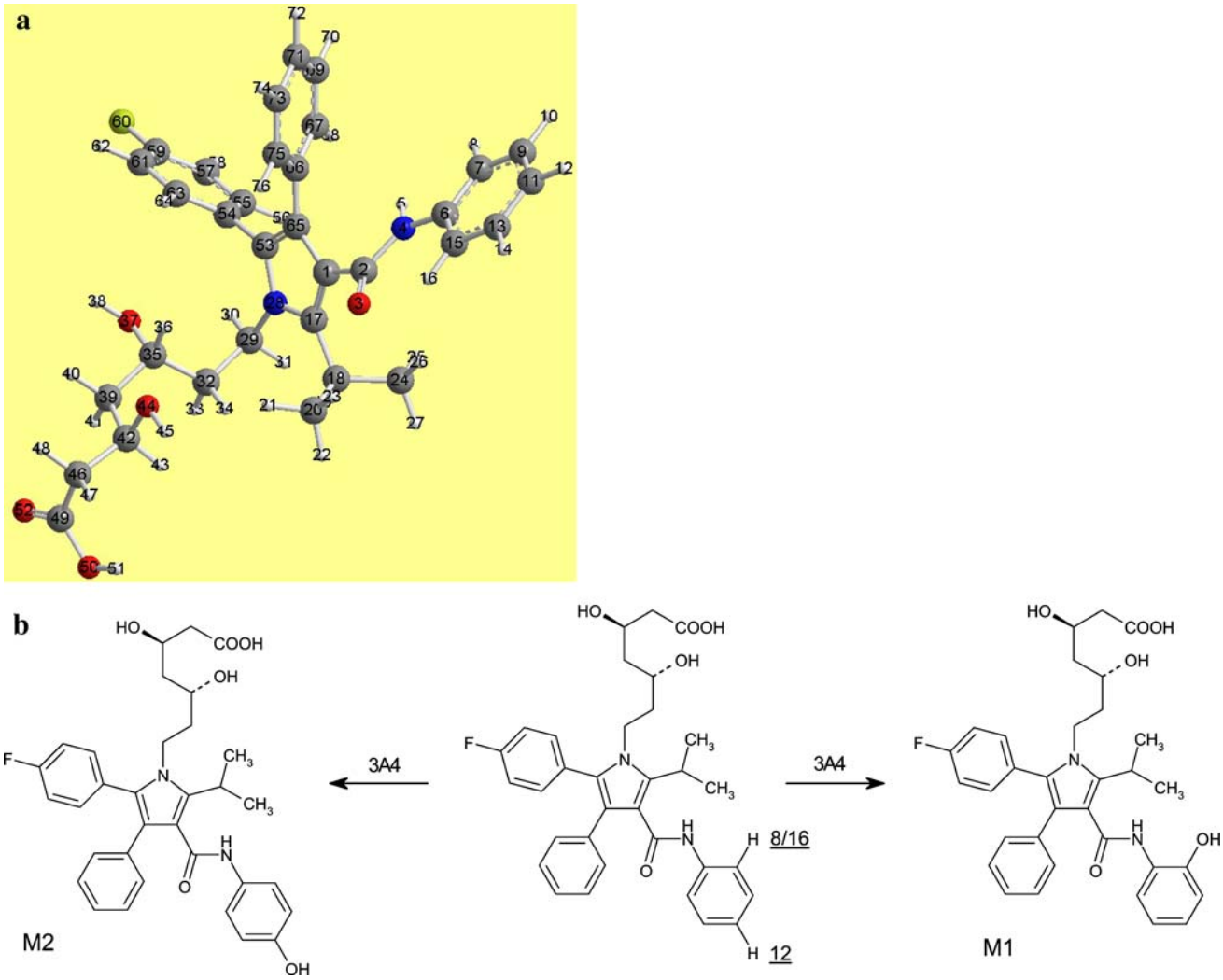

Fig. 1. Atorvastatin. (**a**) 3D averaged structure of atorvastatin (see text for details). (**b**) Experimentally detected metabolites produced by CYP oxidation (40,41). (**c**) The CYP3A4 accessibility (*Ei*, *dark bars*) and probability function *PSMi* (*light bars*) of atorvastatin. (**d**) The CYP3A4 accessibility (*Ei*, *dark bars*) and probability function *PSMi* (*light bars*) of atorvastatin lactone.

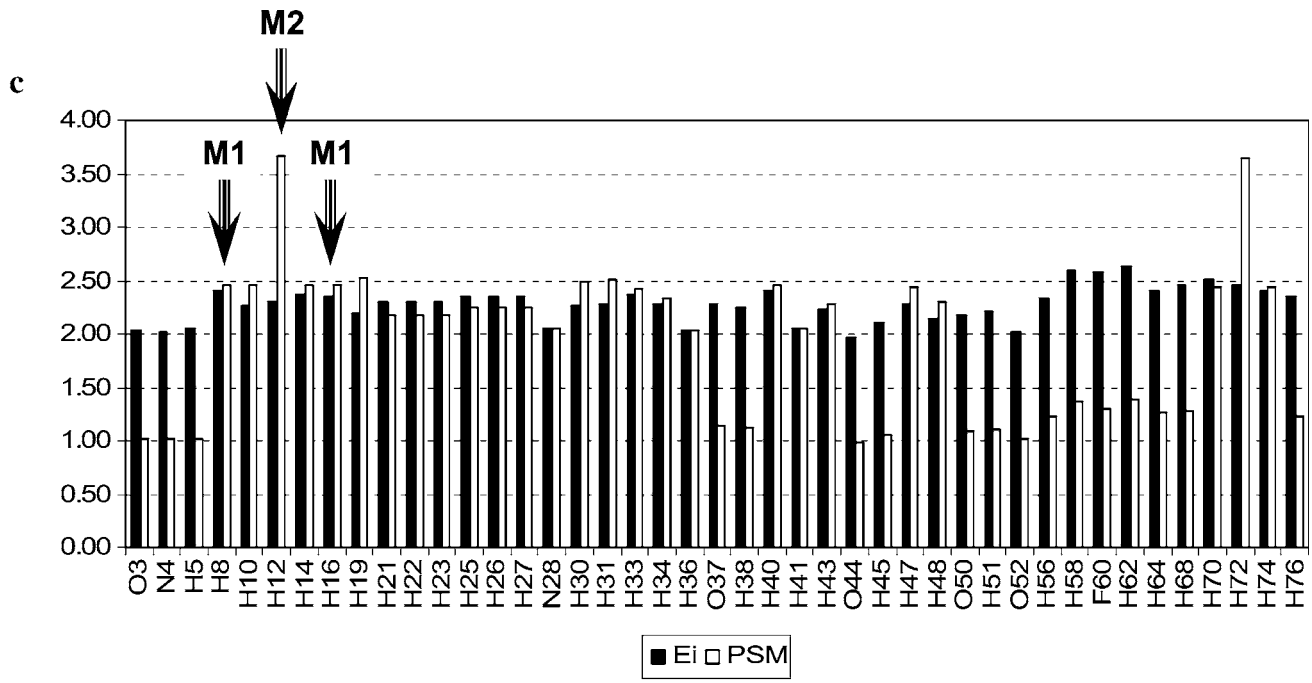

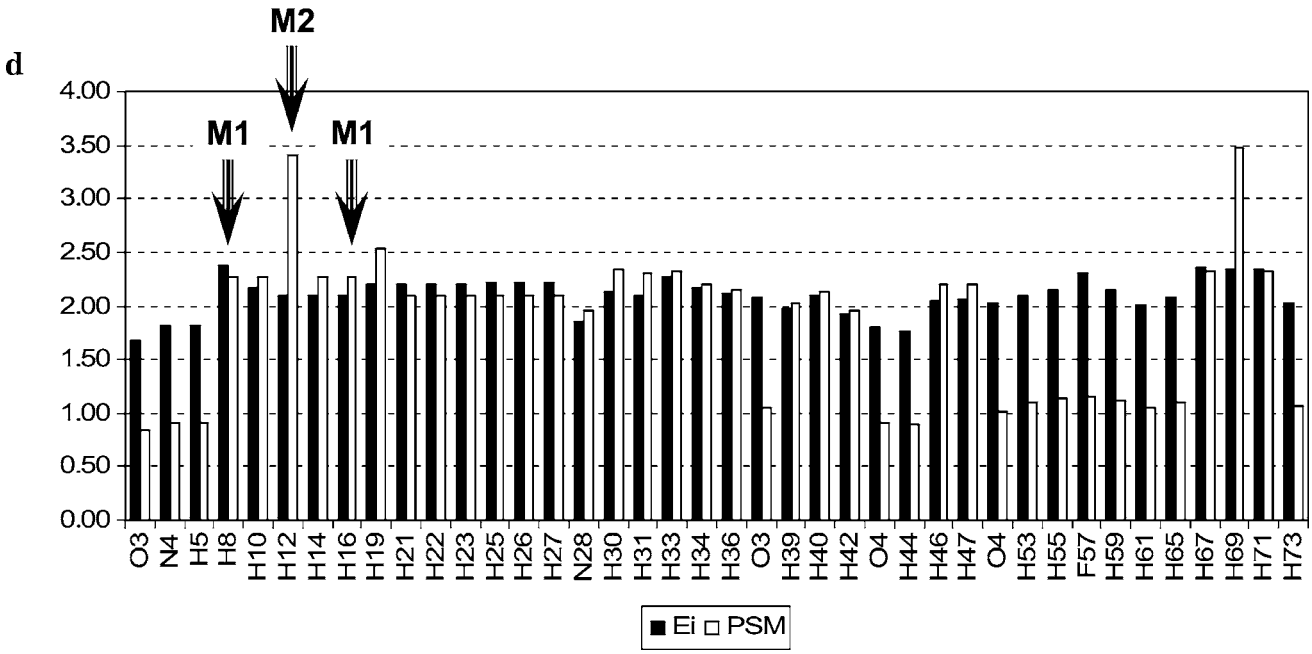

Fig. 1. (Continued).

compared using a similarity analysis method and the atoms of the substrate are ranked according to the accessibility of atom *i* (called recognition score, *Ei*) to the heme. The recognition score *Ei* is then combined with (multiplied by) the chemical reactivity *Ri* (the reactivity of atom *i* toward CYP-oxidation by hydrogen abstraction) to give a probability function $P_{SM}i$ (Eq. 1), namely the probability of atom *i* to be a site of metabolism. This probability function is used to prioritize the potential target sites in the molecule.

$$P_{SM}i = Ei \times Ri \quad (1)$$

In other words, *MetaSite* takes the 3D stereoelectronic structure of both the enzyme and the ligand into account; in contrast, no kinetic or a priori consideration is implemented. *MetaSite* has not been designed to predict metabolic parameters such as K_M or V_{max} or to provide quantitative predictions. And as stated above, its use is currently restricted to the major human CYPs and their oxidative capacity. Finally, MetaSite is not a docking procedure since (a) reactivity is taken into account, and (b) no information is given about the positioning of the substrate in the CYPs binding sites. In principle, it could be possible to replace the recognition component implemented in *MetaSite* with scores obtained from

docking tools but this would cause a dramatic increase in calculation time and introduce the well-known problem of chosing the "best" scoring function (45).

EXPERIMENTAL SECTION

3D-structures (Input)

Because of the absence of any crystallographic data, atorvastatin, cerivastatin fluvastatin and pitavastatin were obtained using the MOE 3D conversion tool (46) from SMILES code and further MMFF94x minimization. For fluvastatin two *erythro* enantiomers were built: the (3R,5S)- and the (3S,5R)-form. The corresponding lactones were built by modifying only the hydroxy-acid moiety and leaving the rest of the molecule unchanged.

Simvastatin (code EJEQAL) and pravastatin (code SAWFIF) were found in the Cambridge Structural Database (CSD, version 5.26, data updates August 2005), saved in the Tripos mol2 format and read in MOE (46) to delete co-crystallized water molecules and add hydrogen atoms. Finally the conformation minimized under MMFF94x (47) conditions was stored and used as *MetaSite* input.

Because of their structural similarity, lovastatin was obtained from simvastatin using the MOE building tool and minimized by MMFF94x force field. Their open analogues were obtained by MOE manipulation of the lactone ring.

Finally, all 3D structures were saved in Tripos mol2 format and Vega molecular modelling package (48) was used for numbering atoms.

MetaSite 2.5.3.

All the statins were submitted to several *MetaSite* runs. The first run was performed on the .mol2 file obtained as described above using *MetaSite* default parameters (i.e., the reactivity contribution (Eq. 1) was included in the calculations) and all CYP models implemented in the software (CYP1A2, CYP2C19, CYP2C9, CYP2D6 and CYP3A4).

The second run was carried out using the same input as above including default parameters, but using two crystallographic CYP models downloaded from the Protein Data Bank (PDB): CYP3A4 (code 1TQN) (26) and CYP2C9 (code 1OG5) (25). The crystallographic data were imported in *MetaSite* and stored for calculation by the ad hoc tool.

The runs for all CYP models were carried out using as input the whole conformer population obtained from both

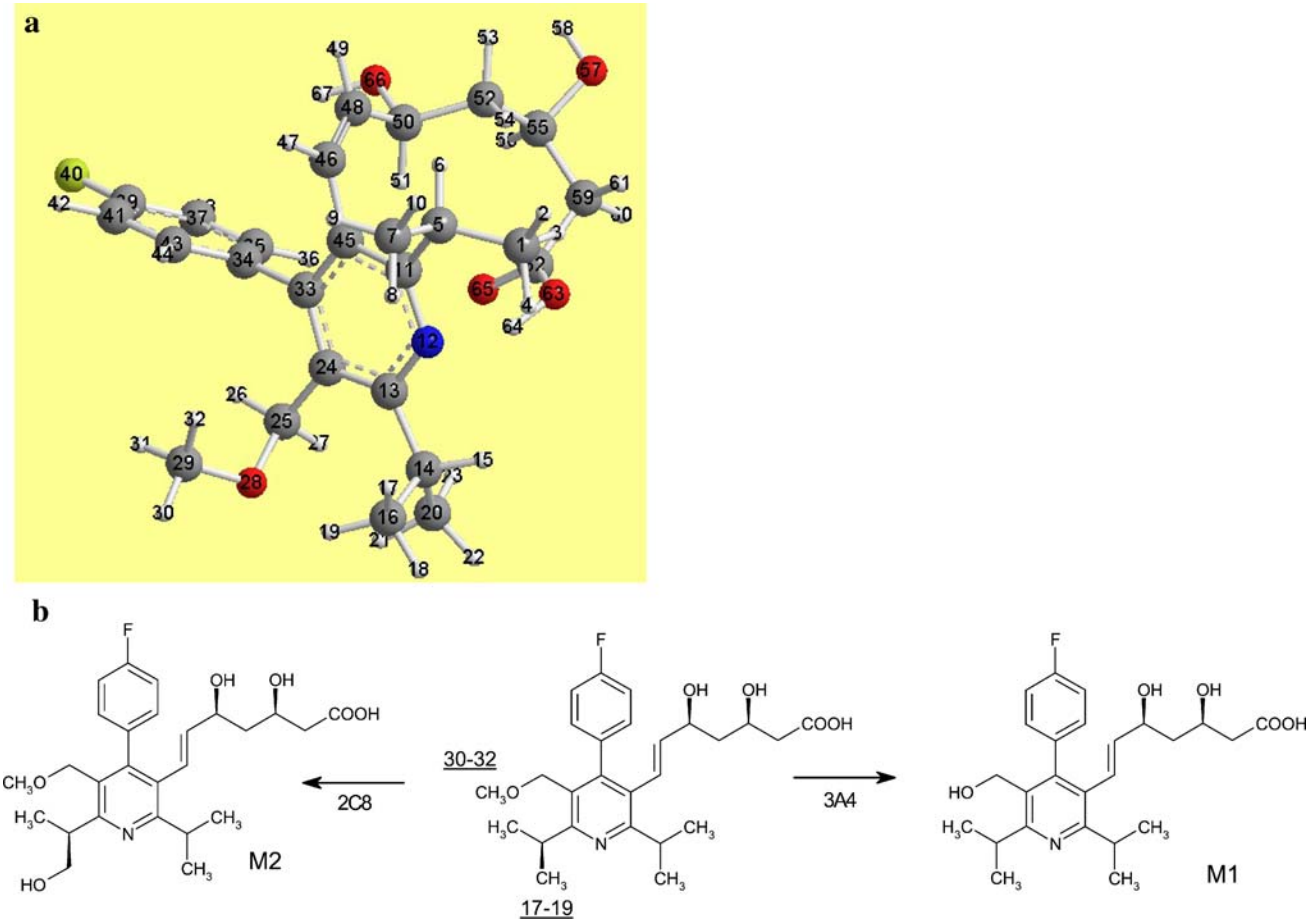

Fig. 2. Cerivastatin. (**a**) 3D averaged structure of cerivastatin (see text for details). (**b**) Experimentally detected metabolites produced by CYP oxidation (57,58,59). (**c**) The CYP3A4 accessibility (*Ei*, *dark bars*) and probability function *PSMi* (*light bars*) of cerivastatin. (**d**) The CYP3A4 accessibility (*Ei*, *dark bars*) and probability function *PSMi* (*light bars*) of cerivastatin lactone. (**e**) The CYP2C9 accessibility (*Ei*, *dark bars*) and probability function *PSMi* (*light bars*) of cerivastatin. (**f**) The CYP2C9 accessibility (*Ei*, *dark bars*) and probability function *PSMi* (*light bars*) of cerivastatin lactone.

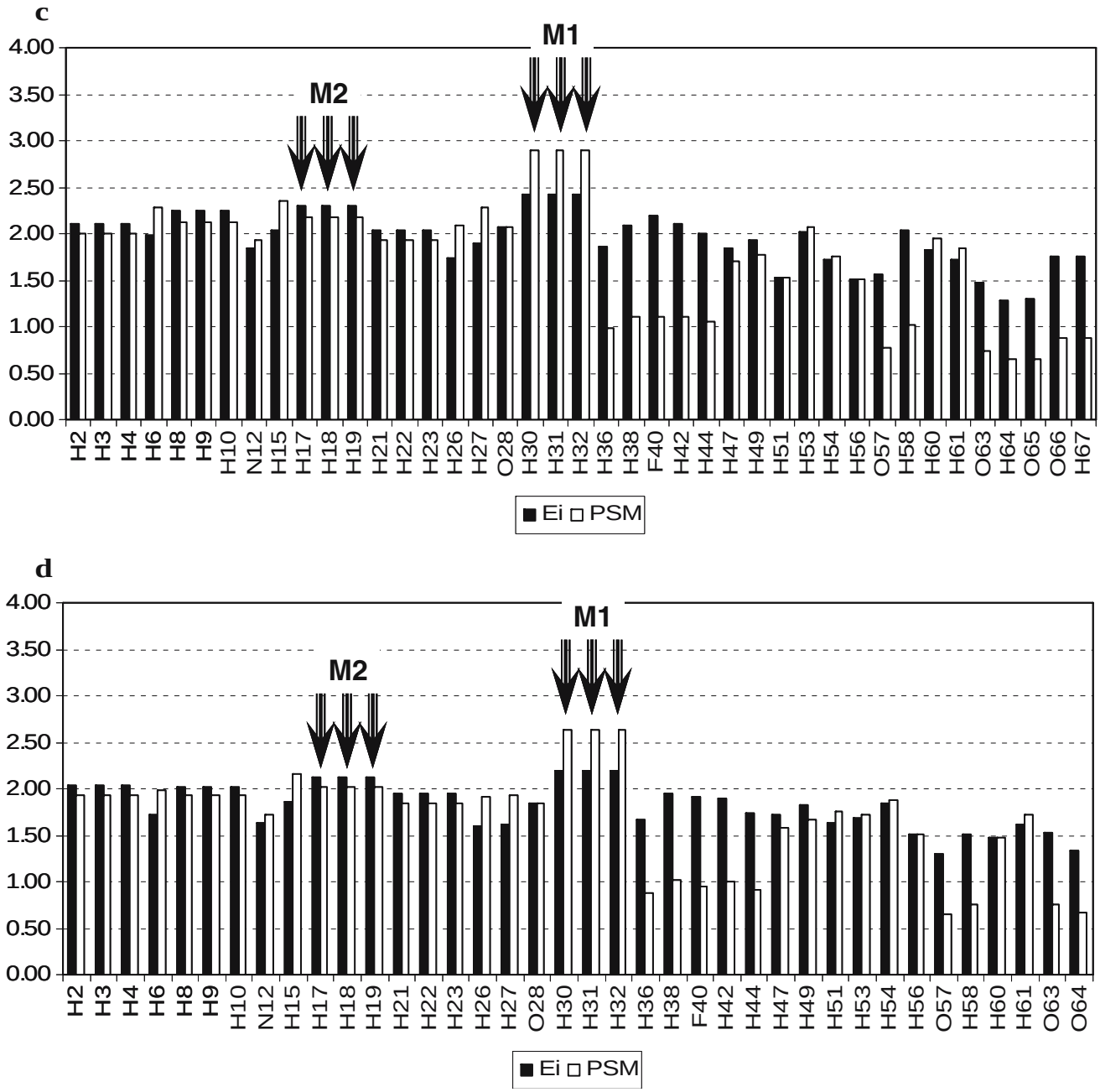

Fig. 2. (Continued).

HMC (see below) and the conformational search algorithm implemented in *MetaSite*. Finally, all runs were repeated by excluding the reactivity part to obtain the accessibility contribution (Eq. 1) alone.

Each *MetaSite* run for about 100 conformers can be performed in a few seconds but data treatment as described below requires about half an hour per ligand/substrate system.

Data Treatment

Since *MetaSite* output is not optimized to extract the full information generated by the software, intermediate results were stored in ASCII files which were read by Excel.

For each molecule two ASCII files were generated: the first contained the $P_{SM}i$ values (i.e., the probability function) and the second the *Ei* values (i.e., the accessibility; Eq. 1) for all atom (Supporting Information) and all CYP models. According to Eq. 1 we were thus able to calculate *Ri* which is not given by the software (Supporting Information).

Molecular Dynamics Simulation

The conformational hypersurface of the compounds was explored using the Hybrid Monte Carlo (HMC) module implemented in MOE as described in detail elsewhere (49).

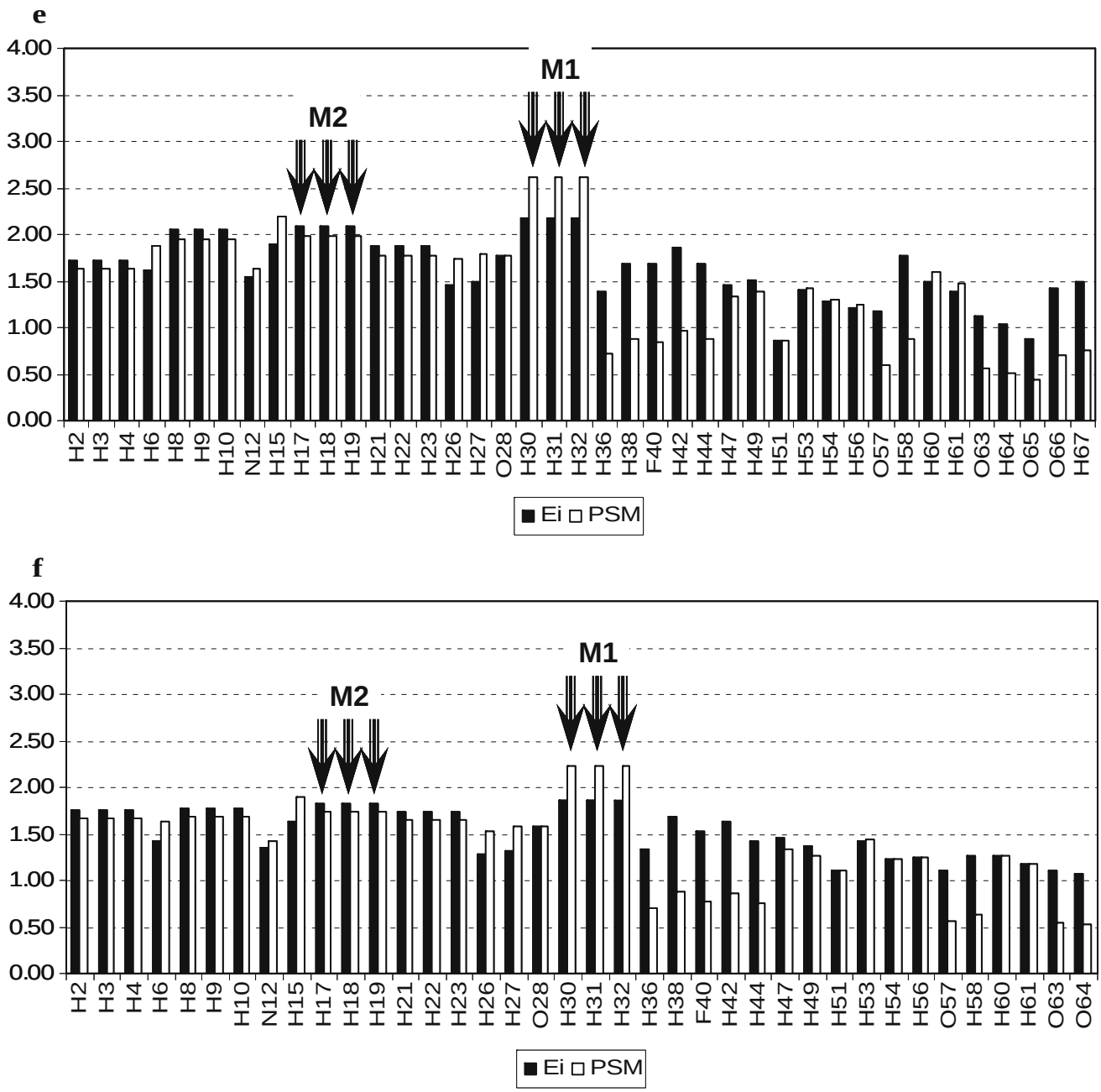

Fig. 2. (Continued).

The HMC conditions were as follows: Iterations=20,000; Save period=100; MD Steps=1, MD Time Step=0.005 ps; Temperature=2,000 K; Equilibration steps=100. Minimization was performed under in vacuo and GB-SA (50) conditions using MMFF94x force field.

The final MOE databases were ranked by energy and exported as mol2 file. The latter were submitted to *MetaSite* without any further modification.

The internal MetaSite conformer generation procedure was also used to obtain a third database of conformers for all the investigated statins. All calculations were performed on a Linux based dual processor Appro1124 server and on standard PCs operating with Microsoft Windows XP.

RESULTS AND DISCUSSION

Overview

The seven statins investigated are atorvastatin, cerivastatin, fluvastatin, pitavastatin and pravastatin which are or were used as the open (hydroxy-acid) form, and lovastatin and simvastatin, which are used as the lactone form. Here, given the lactone/hydroxy-acid equilibrium the drugs undergo in solution and *in vivo* (30,32) and the recently reported affinities of both forms for specific CYPs (51), the seven statins were investigated twice, in their lactone form and in their hydroxy-acid form. This created a minor problem with

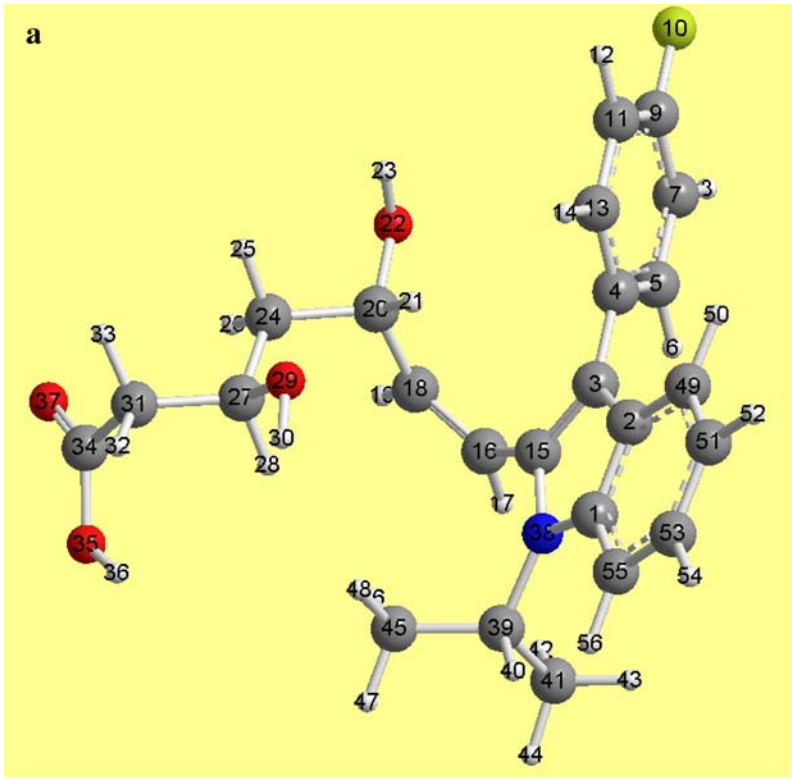

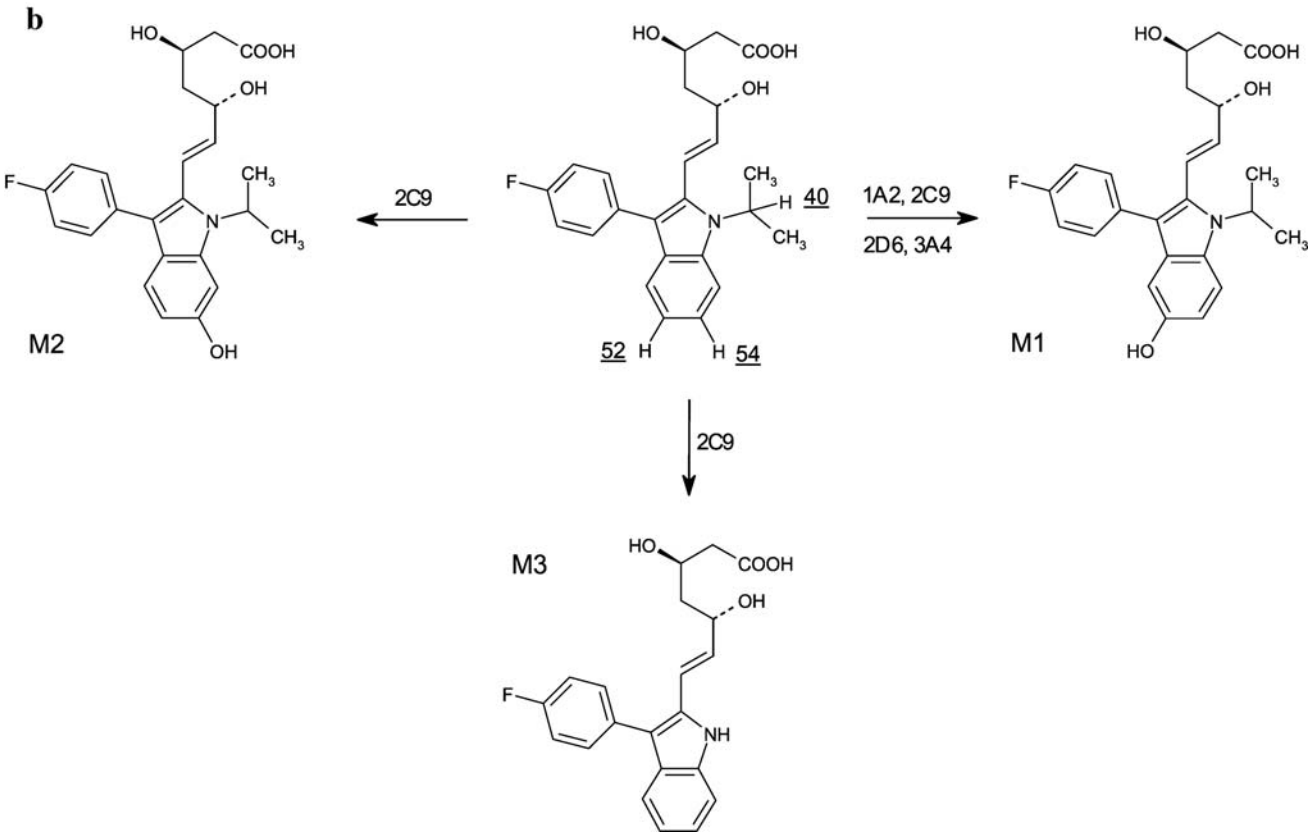

Fig. 3. Fluvastatin. (**a**) 3D averaged structure of fluvastatin (see text for details). (**b**) Experimentally detected metabolites produced by CYP oxidation (40,41). (**c**) The CYP2C9 accessibility (*Ei*, *dark bars*) and probability function *PSMi* (*light bars*) of fluvastatin. (**d**) The CYP2C9 accessibility (*Ei*, *dark bars*) and probability function *PSMi* (*light bars*) of fluvastatin lactone.

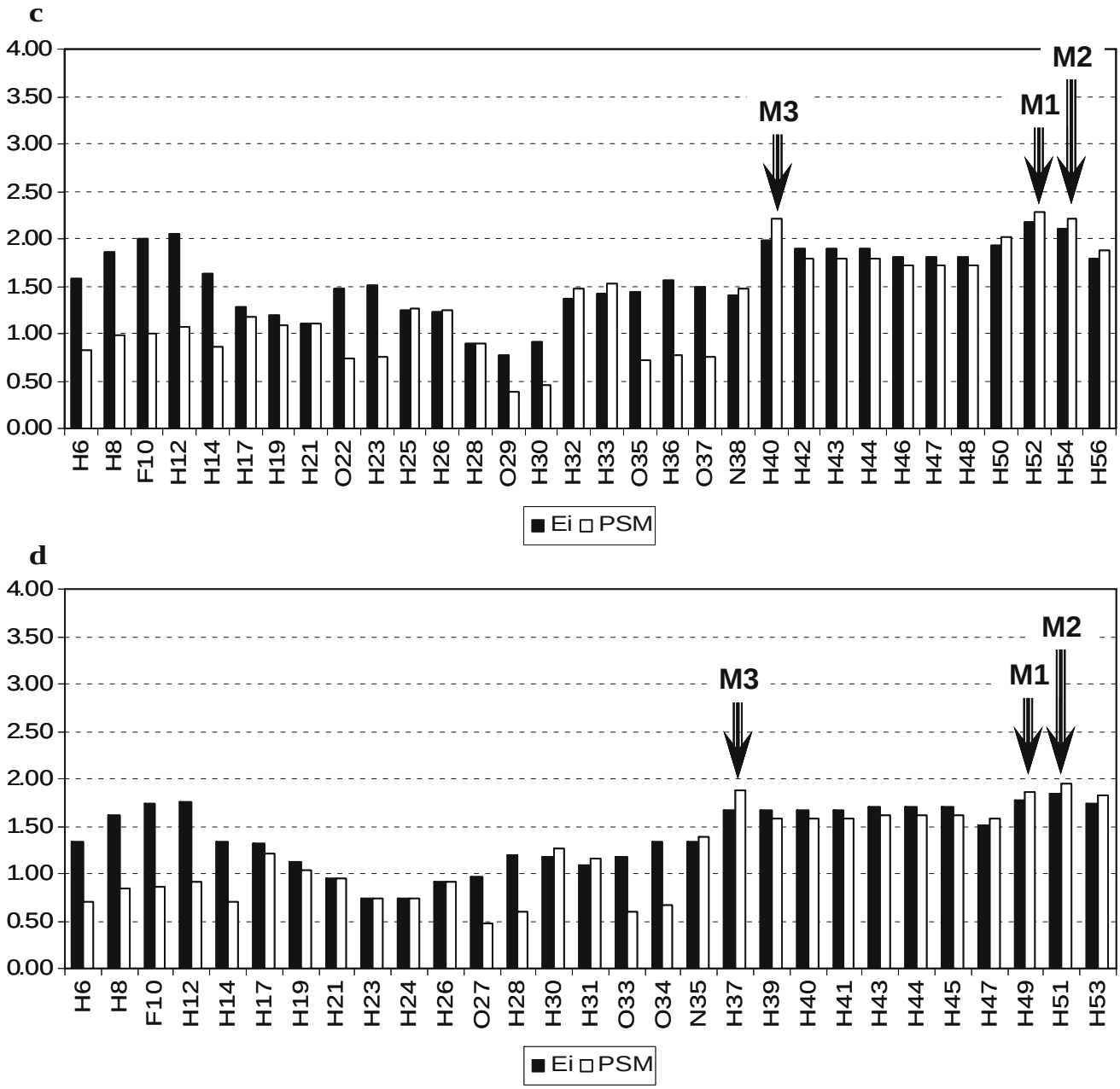

Fig. 3. (Continued).

the automatic atom numbering, as some corresponding atoms did not have the same number.

To better interpret the metabolic predictions and to improve on the standard *MetaSite* procedure, we also calculated separately the recognition score *Ei* and the chemical reactivity *Ri* besides P_{SM} (see Experimental Section and Supporting Material).

In principle, to establish an objective criterion to measure the predictive power of *MetaSite*, the user should be able to define a general threshold value of P_{SM} able to distinguish between high and low probability sites of metabolic attack. However, the assumptions in *MetaSite* (e.g., the molecule must be able to reach the iron heme) render impossible a quantitative comparison of E_i (and thus P_{SM}) values between different molecules, and between different CYPs structures for the same molecule.

In a very interesting paper, Zhou *et al.* (38) recently proposed that the validation of the *MetaSite* predictions could be obtained by counting the number of experimentally reported metabolic pathways found among the first, second, and third sites as ranked by *MetaSite*. Since the number of sites to be considered is questionable, we simply examined here how each experimental metabolite was ranked by *MetaSite*. A global view of results for CYP3A4 and CYP2C9 (the two most relevant isoenzymes involved in the metabolism of statins) is given in Table I. The results indicate that in 77% of cases, the experimental metabolites are ranked from the first to the fifth most probable by *MetaSite* based on its

built-in homology model. In other words, *MetaSite* offers both correct predictions and false positives (metabolites not seen experimentally). False negatives (non-prediction of actual metabolites) are also seen, although defining a false negative is difficult with *MetaSite* unless a cut-off is arbitrarily defined. In our view, false positives should not be discounted since they may be of interest by hinting at minor and as yet unidentified metabolites, or by pointing to a potentially labile site whose actuality is not realized due to various biological factors. Interestingly, a success rate of 82% for this small series of congeneric drugs is in good agreement with the original validation performed by Cruciani *et al*. on an extended database of chemicals (40).

In this study we used two distinct 3D-models for CYP2C9 and CYP3A4, namely the models implemented in the software and X-ray models downloaded from the Protein Data Bank (PDB) (see Experimental Section). Table I demonstrates that predictions obtained by homology models are slightly better than those obtained from the crystallographic structures of CYPs, the difference being of modest here.

The influence of substrate flexibility on the predictions was also analyzed. In this study, however, the starting conformer was found to be representative of the whole population of conformers, implying that flexibility does not seem to influence the oxidative metabolism of statins.

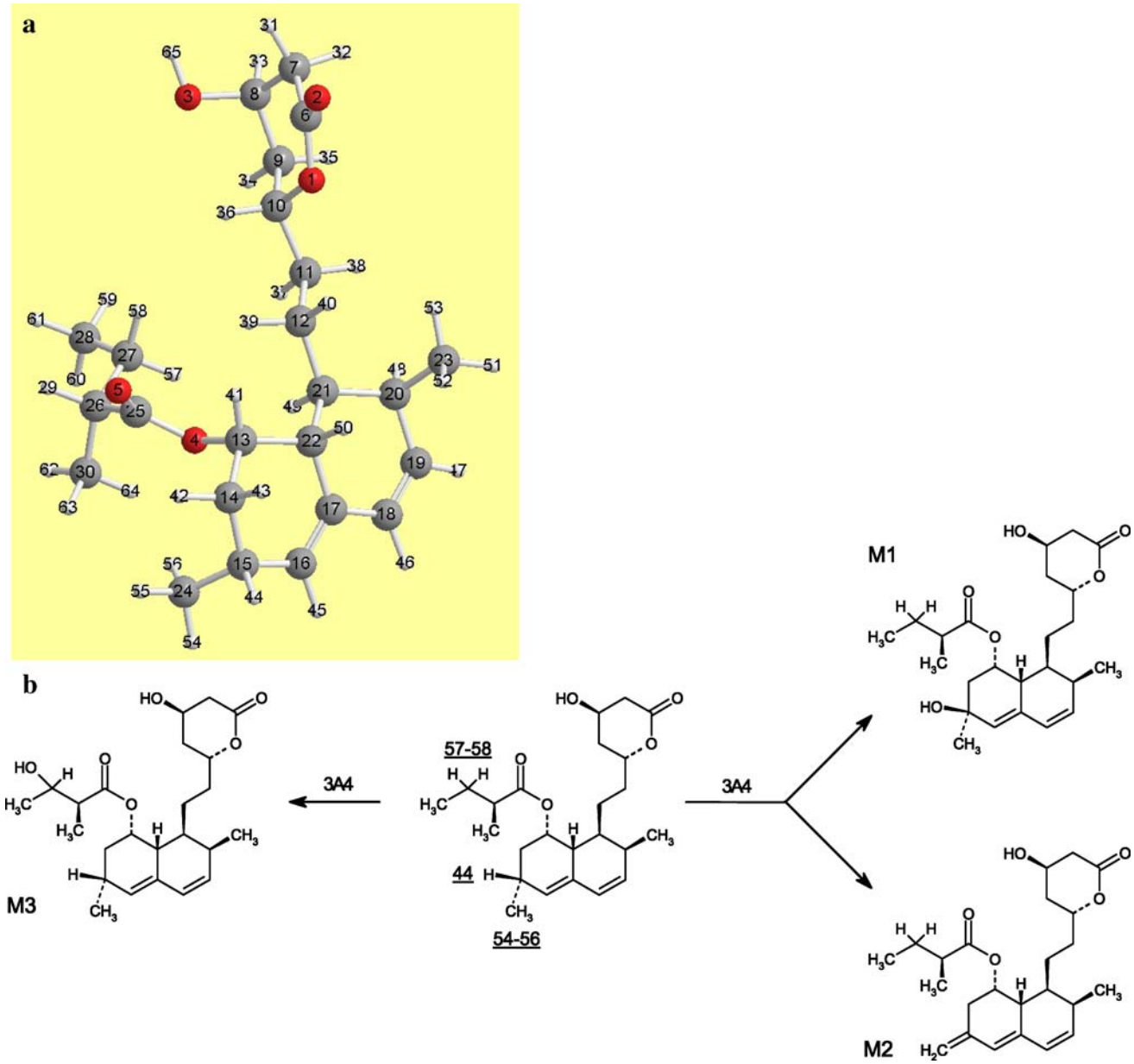

Fig. 4. Lovastatin. (**a**) 3D averaged structure of lovastatin (see text for details). (**b**) Experimentally detected metabolites produced by CYP oxidation (40,41). (**c**) The CYP3A4 accessibility (*Ei*, *dark bars*) and probability function *PSMi* (*light bars*) of lovastatin. (**d**) The CYP3A4 accessibility (*Ei*, *dark bars*) and probability function *PSMi* (*light bars*) of lovastatin (hydroxy-acid form).

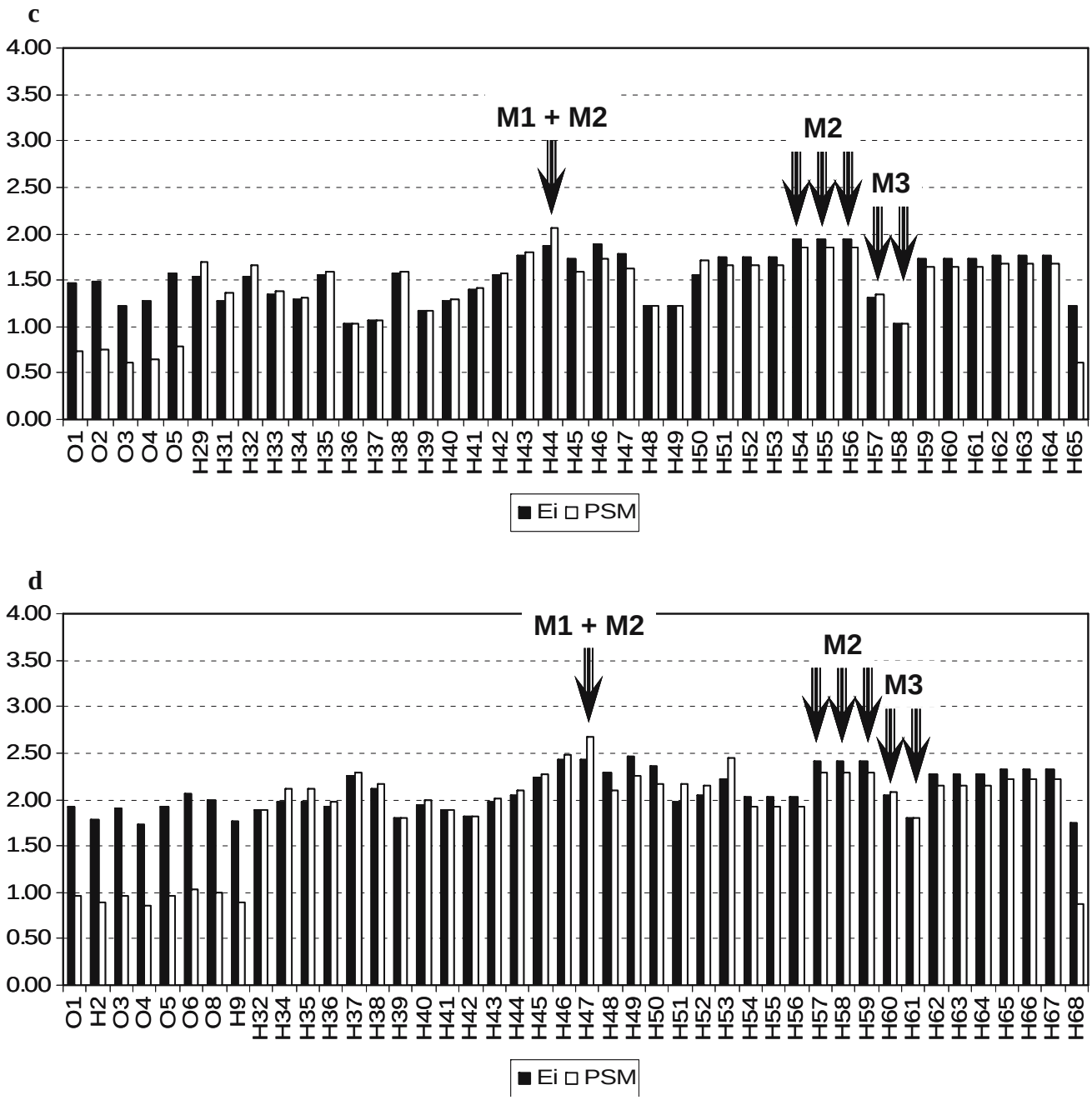

Fig. 4. (Continued).

We now discuss in turn the results for the individual statins taken in alphabetical order.

Atorvastatin

Like other statins, atorvastatin ((*βR*,*δR*)-2-(4-fluorophenyl)-*β*,*δ*-dihydroxy-5-(1-methylethyl)-3-phenyl-4-((phenylamino)carbonyl)-1*H*-pyrrole-1-heptanoic acid) undergoes extensive first pass metabolism. An averaged 3D structure is shown in Fig. 1a (see the Experimental Section for details).

As extensively reviewed, (36,37) atorvastatin is metabolized mainly by CYP3A4, but studies with human liver microsomes suggest that a step preceding oxidation is lactonization, since the lactone appears to be the relevant CYP substrate. Two main metabolites have been identified, namely the *ortho*-hydroxy and *para*-hydroxy metabolites (*M1* and *M2*, respectively, in Fig. 1b). These positions of metabolic attack correspond to C7/15 (hydrogen atoms H8/16) and C11 (H12), respectively; these numbers remain unchanged in the lactone form. It is also worthwhile noting that these metabolites make a major contribution to the activity of atorvastatin.

Using the averaged conformer as an input, *MetaSite* offered a large number of predictions (Fig. 1c for the hydroxy-acid form, Fig. 1d for its lactone metabolite). As can be seen, H12 (which corresponds to metabolite *M2*) was

predicted as the most probable metabolite (Table I). The positions H8/16 (which correspond to *M1*) are predicted with a fair probability function (position 9, see Table I). But so are a number of other positions which do not correspond to identified metabolites and await possible experimental confirmation. In other words, *MetaSite* like all other algorithms or platforms of this type can only suggest probable sites and thereby help bioanalysts elucidate structures, but they cannot replace experimental investigations.

The case of the aromatic para-position H72 (H69 in the lactone) is of particular interest as it appears as a false positive (position 2). *MetaSite* assigned this position as the most probable sites of oxidation together with H12 (i.e., *M2*). This was confirmed when taking flexibility into account (data not shown), with H72/69 remaining the prime metabolic position and H12 the second one. It is intriguing to note that the two *ortho*- and the two *meta*-positions on the anilidino ring (8 or 16, and 10 or 14, respectively) received the same probability score when it is well-known that *meta*-positions are seldom hydroxylated. In fact, H8 and H16 have a higher recognition score *Ei* than H10 and H14, in agreement with the CYP3A4 production of the *ortho*-phenol (metabolite *M1*), a higher recognition score exactly compensated by a distinctly lower chemical reactivity *Ri*. This would suggest that the chemical reactivity score implemented in *MetaSite* is not fully relevant to the biochemical mechanism of CYP-catalyzed aryl oxidation where H-abstraction is not the rate-limiting step (52).

Predictions comparable to those in Fig. 1c and d were obtained with the models for CYP1A2, 2C9 and 2C19 (results not shown). Furthermore, the two X-ray structures (CYP2C9 and 3A4) showed a better metabolic capacity toward atorvastatin than the standard 3D structures used by *MetaSite* and based on homology modeling.

Cerivastatin

An averaged 3D structure is shown in Fig. 2a (see the Experimental Section for details).

Cerivastatin has been withdrawn from the market but it remains a metabolically interesting substrate (Fig. 2a). It undergoes two main CYP-catalyzed oxidations in humans, namely O-demethylation to generate *M1*, and a product stereoselective aliphatic hydroxylation to yield *M2* (53). These positions of metabolic attack correspond to C29 (hydrogen atoms H30–32) and C16 (H17–19), respectively. The former reaction is catalyzed mainly by CYP3A4, and the latter by CYP2C8 (54).

The *MetaSite* predictions are comparable for the various CYP models, with a consistent and marked preference for positions H30–32, i.e., O-demethylation. This is a valuable result (Fig. 2c and d) given that the O-demethylated metabolite is indeed a major metabolite not only in humans, but also in dogs, rats and mice (55). The second position (Table I) is assigned to the methine group in the isopropyl substituent, but this reaction does not appear to have been seen experimentally. Remarkably, the CYP2C9 (Fig. 2e and f) and other models predict a high probability of hydroxylation (3rd rank in Table I based on the CYP2C9 model) at a methyl group in the isopropyl substituent, with a visible preference for the *pro-S* methyl group (C16 and H17–19 rather than C20 and H21–23). This is indeed what was found experimentally with *M2*. To the best of our knowledge, this is the first time that a metabolite is predicted with product stereoselectivity (discrimination between two enantiotopic or diastereotopic positions).

Fluvastatin

Fluvastatin, (±)-(3R*,5S*,6E)-7-(3-p-fluorophenyl)-1-isopropylindol-2-yl)-3,5-dihydroxy-6-heptenoic acid, is the first fully synthetic HMG-CoA reductase inhibitor. The commercial form includes a racemate of the two *erythro* enantiomers with the (3*R*, 5*S*)-form possessing more than 30 times the activity of the (3*S*, 5*R*) form (36,37). The most active enantiomer (Fig. 3a) was constructed as described in the Experimental Section.

According to available experimental studies, (35,36,37) fluvastatin is metabolized by cytochromes P450 to three primary metabolites (Fig. 3b). These are 5-hydroxyfluvastatin (*M1*), 6-hydroxyfluvastatin (*M2*), and *N*-deisopropylfluvastatin (*M3*). Like for several other statins, β-oxidation is also a significant pathway, (35) but this is not relevant to CYP-catalyzed metabolism. CYP2C9 is believed to be the exclusive enzyme involved in the formation of *M2* and *M3* in humans, whereas 5-hydroxyfluvastatin (*M1*) is also formed by CYP1A2, 2D6 and 3A4 (36,37). The two hydroxylated compounds (*M1* and *M2*) are active but undergo rapid elimination.

As far as aromatic oxidation is concerned, the CYP2C9 model in *MetaSite* gave the highest priority to C51 (H52) and C53 (H54) (Fig. 3c), and indeed H52 and H54 correspond to *M1* and *M2*. The next aromatic position predicted, C49 (H50), is not confirmed by currect experimental data. And the reaction of N-dealkylation (corresponding to H40 abstraction) was a clear and correct prediction. All these sites were predicted based on a combination of higher chemical reactivity and proper alignment in the catalytic site (recog-

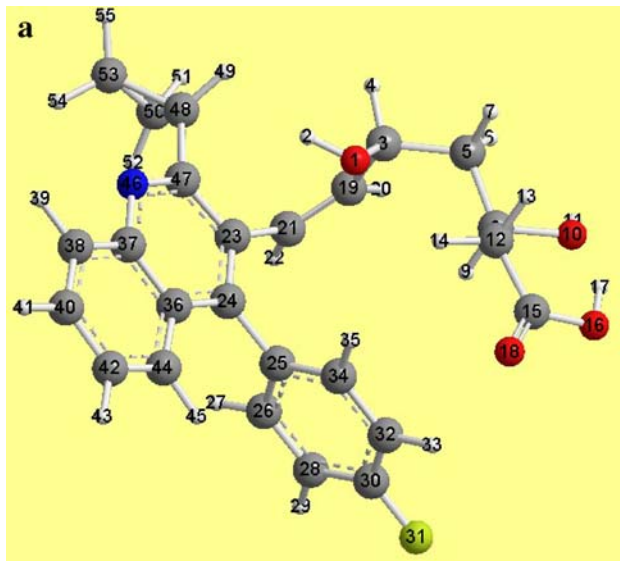

Fig. 5. Pitavastatin. (**a**) 3D averaged structure of pitavastatin (see text for details). (**b**) Experimentally detected metabolites produced by CYP oxidation (62). (**c**) The CYP3A4 accessibility (*Ei*, *dark bars*) and probability function *PSMi* (*light bars*) of pitavastatin. (**d**) The CYP2C9 accessibility (*Ei*, *dark bars*) and probability function *PSMi* (*light bars*) of pitavastatin. (**e**) The CYP2D6 accessibility (*Ei*, *dark bars*) and probability function *PSMi* (*light bars*) of pitavastatin lactone.

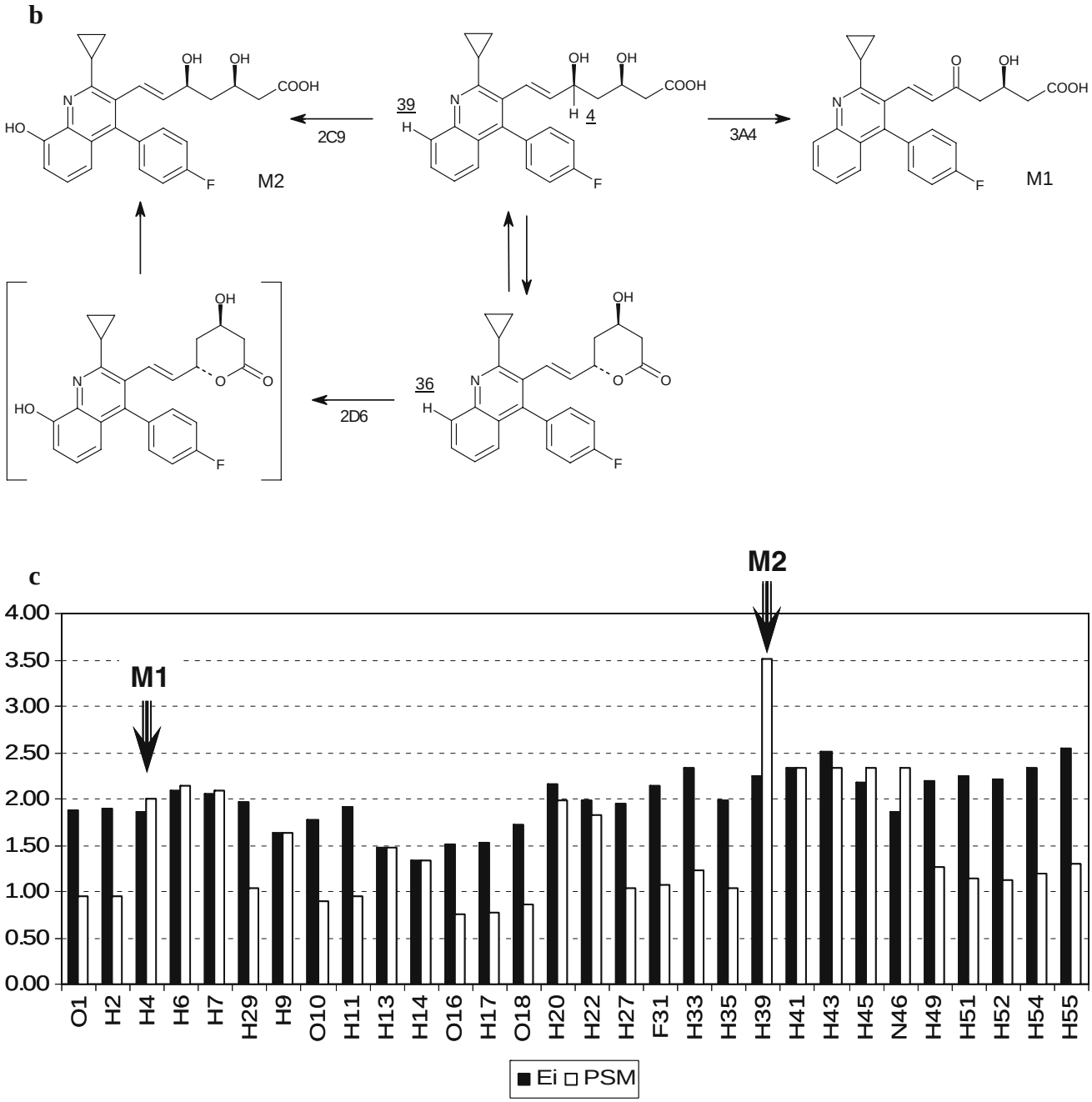

Fig. 5. (Continued).

nition score). A similar conclusion emerges for the lactone form, although the results are slightly less clear-cut (Fig. 3d).

The formation of *M1* from CYP1A2 and 3A4 was also predicted by their respective *MetaSite* models, but so were the other known metabolites. The 2D6 model suggested a low accessibility (results not shown).

In principle one could expect that *MetaSite* suggests the CYP mainly involved in a given reaction (e.g., *M2* should receive a higher rank in the 2C9 prediction and a lower one with the other CYP models) but this is not within the capabilities of the current versions of *MetaSite*.

MetaSite applied to the less active enantiomer gave results similar to the most active one (results not shown).

Lovastatin

Lovastatin, (1*S*,3*R*,7*S*,8*S*,8a*R*)-1,2,3,7,8,8a-hexahydro-3,7-dimethyl-8-(2((2*R*,4*R*)-tetrahydro-4-hydroxy-6-oxo-2*H*-pyran-2-yl)ethyl)-1-naphthalenyl (2*S*)-2-methylbutanoate, is a natural lactone prodrug (like simvastatin) derived from the fungus *Aspergillus terreus* which is converted in the gastrointestinal tract, plasma and liver to the active hydroxy-acid form (36,37). An averaged 3D-structure obtained by modification of the X-ray structure of simvastatin is shown in Fig. 4a (see Experimental Section for details).

Lovastatin is oxidized in human liver microsomes to three known primary metabolites (Fig. 4b), namely 6′β-

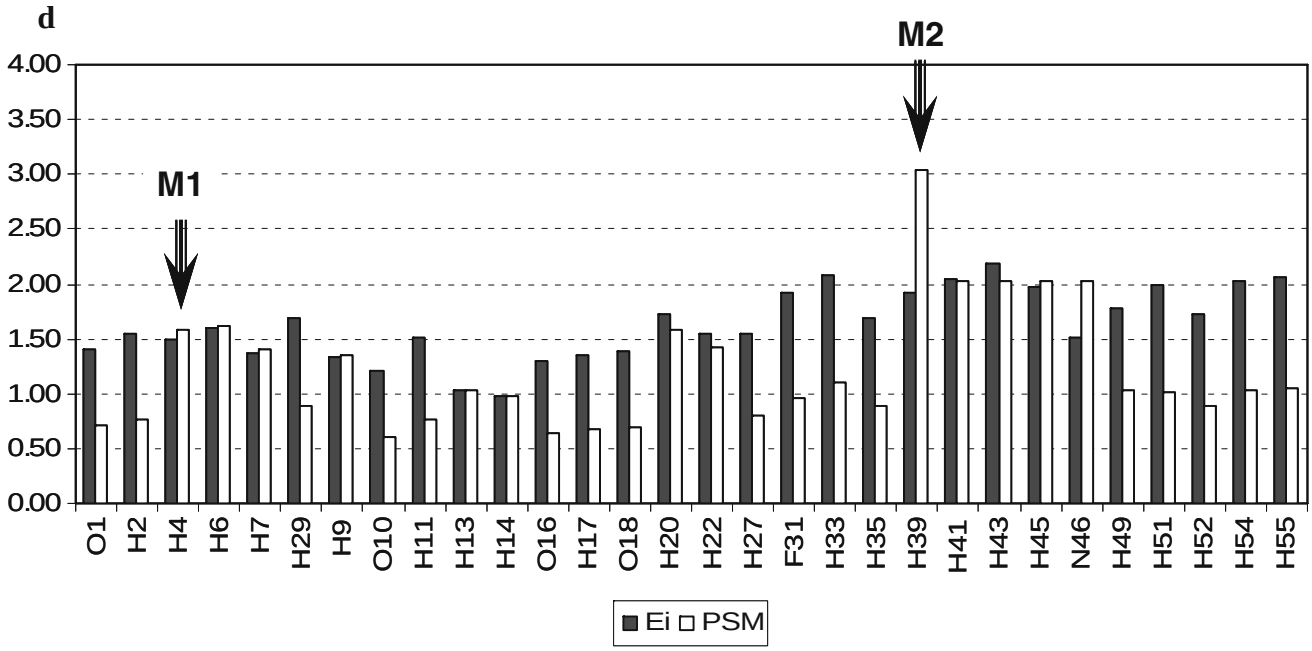

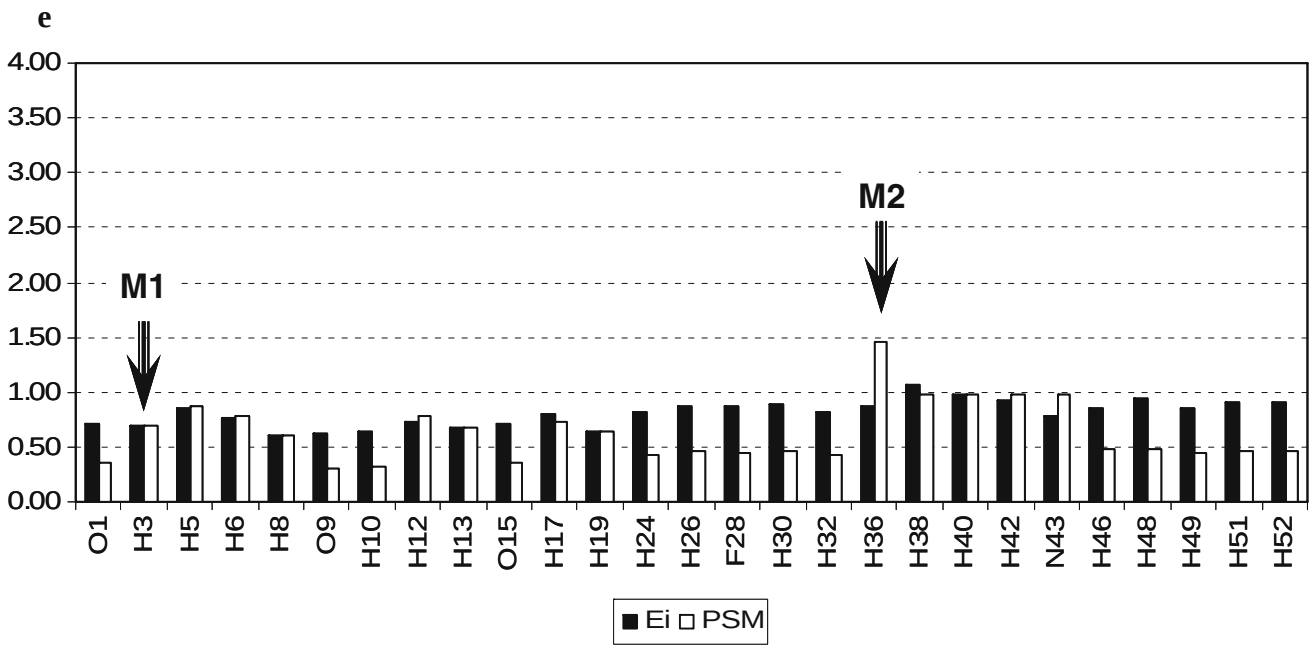

Fig. 5. (Continued).

hydroxylovastatin (*M1*), 3″β-hydroxylovastatin (*M3*), and the 6′-exomethylene metabolite (*M2*). (36,37,56) It is probable although not demonstrated that *M1* and *M2* derive from a single metabolic intermediate formed by H44 abstraction, as evidenced for the allylic oxidation of other substrates. (57) Lovastatin is a substrate of CYP3A enzymes, particularly CYP3A4. The three metabolites in Fig. 4c retain pharmacological activity.

The *MetaSite* predictions for the sites of CYP3A4-catalyzed C-oxidation of lovastatin (i.e., the lactone form) are shown in Fig. 4c. The 6-position (C15–H44) which leads to the formation of *M1* and presumably *M2* was indeed confirmed as the first priority for CYP3A4. Nevertheless, it is interesting to note that C24 (H54, H55 or H56) which could also account for the formation of *M2* received an almost as high priority. In contrast, C27 (H57 or H58, one of either hydrogen to be abstracted during formation of *M3*) was of low priority. A comparable picture emerges from Fig. 4d where the predicted sites of CYP3A4-catalyzed C-oxidations of lovastatin hydroxy-acid are shown. Interestingly, the two geminal H60 and H61 (labeled H57 and H58 in the lactone) are not equivalent due to a different accessibility. In both the lactone and open forms, however, metabolite *M3* is given a low priority.

Since the conformation of flexible substrates with multiple sites of metabolism could have an impact on *MetaSite* predictions, conformational effects were also taken into account. In particular, a number of conformational analyses were tested to overcome artefacts due to procedure (see Experimental Part). The results can then be analyzed by examining one conformer at a time, and/or by analyzing conformational averages (*MetaSite* indeed provides an averaged ranking output which represents a weighted arithmetic mean of atom *i* ranks). Here, both approaches confirmed the low tendency of the lateral chain of lovastatin to be oxidized to *M3*. Taken globally, the *MetaSite* results of lovastatin yield some valuable and some less convincing prioritization of the major human metabolites. Furthermore, the CYP2C9 model gave comparable predictions (results not shown), demonstrating that the current version of *MetaSite* works best when preliminary experimental data are available.

Pitavastatin

The new HMG-CoA reductase inhibitor pitavastatin is of metabolic interest on more than one account. Its 3D-structure (Fig. 5a) was constructed as described in the Experimental Section.

Pitavastatin undergoes a variety of metabolic reactions including lactonization, oxidations and glucuronidations (58). Its CYP-catalyzed metabolism (Fig. 5b) results in two main products. Metabolite *M1* is a ketone produced by the oxidation of a secondary alcohol group. Such a reaction is often mediated by alcohol dehydrogenases, but cytochromes P450 are also known to catalyze alcohol oxidation to carbonyls

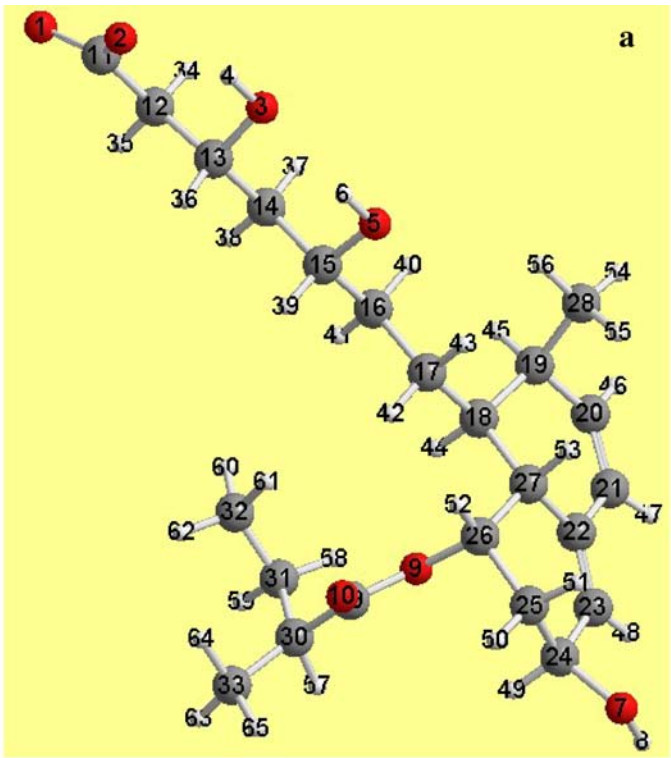

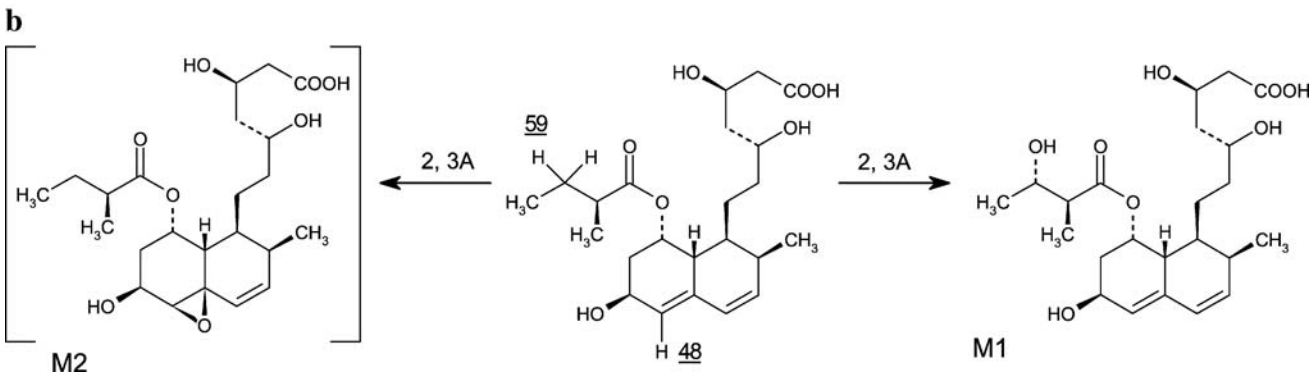

Fig. 6. Pravastatin. (**a**) Crystallographic structure of pravastatin (see text for details). (**b**) Experimentally detected metabolites produced by CYP oxidation (41,64). (**c**) The CYP3A4 accessibility (*Ei*, *dark bars*) and probability function *PSMi* (*light bars*) of pravastatin. (**d**) The CYP3A4 accessibility (*Ei*, *dark bars*) and probability function *PSMi* (*light bars*) pravastatin lactone.

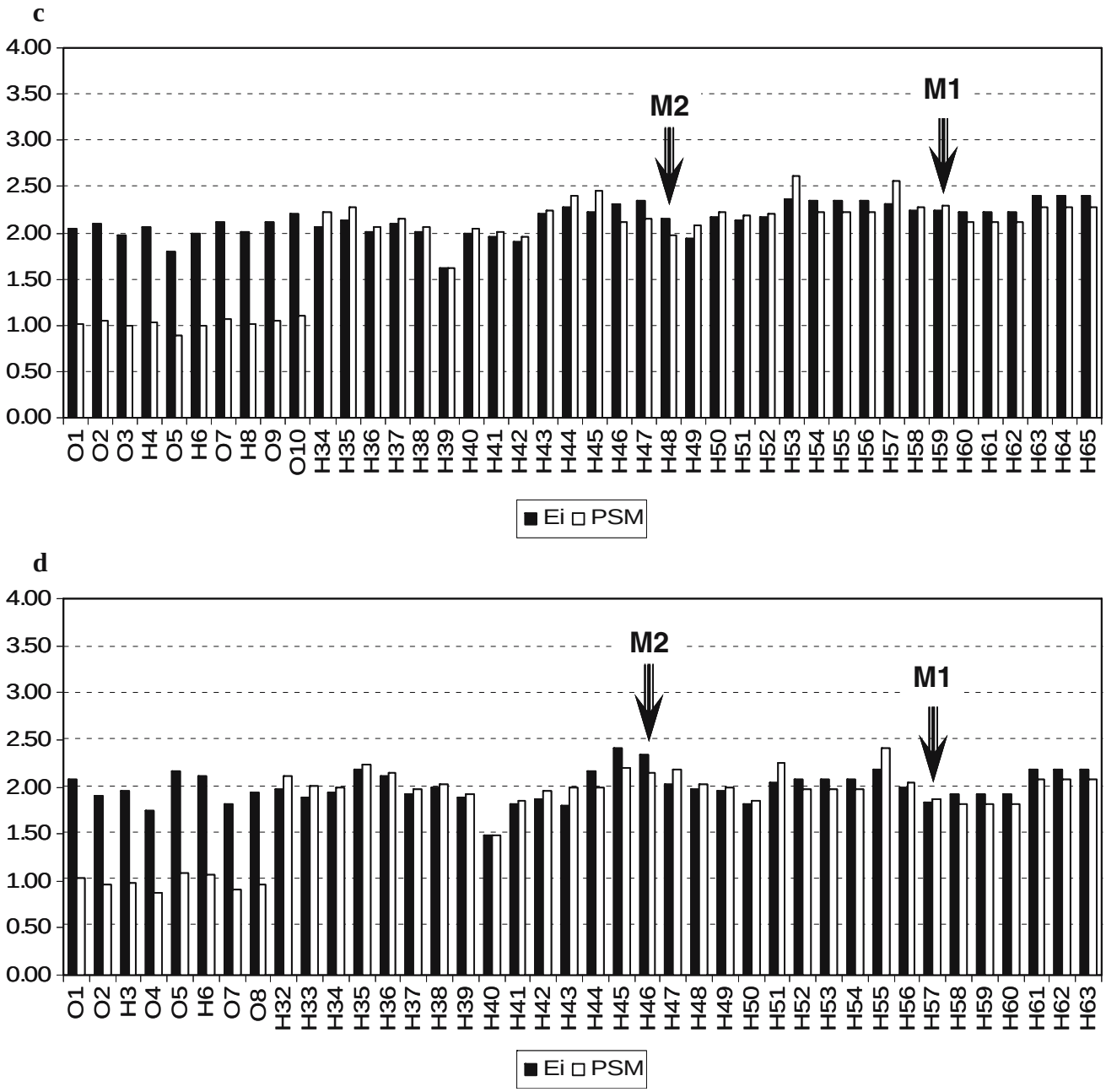

Fig. 6. (Continued).

(59). Here indeed, CYP3A4 was shown to account for this reaction, whose mechanism implies hydroxylation at C3 (i.e., hydrogen H4 abstraction) followed by loss of H_2O from the geminal diol. The second relevant metabolite is the phenol *M2* (oxidation of C38 bearing H39). This reaction is catalyzed by CYP2C9 and 2C8, but there is also an experimental suggestion that the same metabolite can be formed by 2D6 from the lactone (C35 bearing H36) (58).

MetaSite calculates that the primary position of CYP3A4 attack is H39 (leading to *M2*) (Fig. 5c). The secondary sites are the heterocyclic nitrogen (N46) and the three other available positions on the naphthyridine ring (H41, H43 and H45). The H4 position leading to *M1* is given a lower priority in the 3A4 model (Fig. 5c) and most other models.

In all models, positions H39 is indeed calculated to be the primary site of hydroxylation due to its high accessibility and reactivity, thus confirming *M2* as the primary metabolite (see Fig. 5d for CYP2C9). This prediction also holds true for the CYP2D6-catalyzed oxidation of the lactone (see Fig. 5e), where position H36 is clearly the preferred one in agreement with experimental findings (58).

Pravastatin

The 3D-structure of pravastatin (Fig. 6a) was obtained from the CSD (see Experimental Section).

The metabolism of this drug is a complex one involving various enzymes and pathways, in particular CYP-catalyzed

oxidations, β-oxidation, lactonization, hydration, conjugation with glucuronic acid and glutathione, and non-enzymatic rearrangements (37,60). As a result, the evidence for the formation of some metabolites is indirect and must be deduced from their further products. Despite the difficulty of disentangling the various enzymatic and non-enzymatic contributions, two first-generation metabolites appear as clearly due to CYP catalysis (Fig. 6b). Hydroxylation at

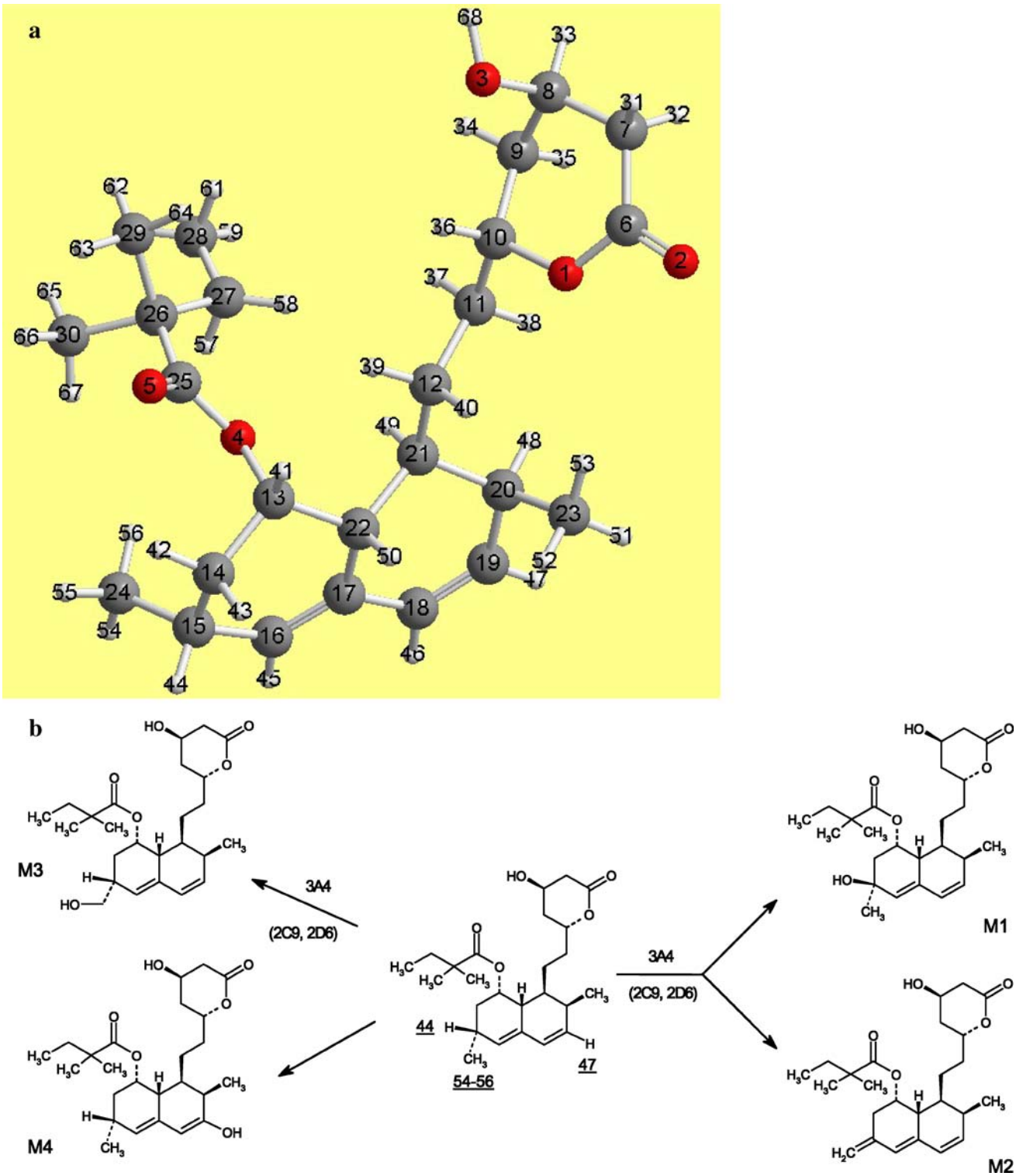

Fig. 7. Simvastatin. (**a**) Crystallographic structure of simvastatin (see text for details). (**b**) Experimentally detected metabolites produced by CYP oxidation (40,41). (**c**) The CYP3A4 accessibility (*Ei*, *dark bars*) and probability function *PSMi* (*light bars*) of simvastatin. (**d**) The CYP3A4 accessibility (*Ei*, *dark bars*) and probability function *PSMi* (*light bars*) of simvastatin (hydroxy-acid form). (**e**) The CYP2C9 accessibility (*Ei*, *dark bars*) and probability function *PSMi* (*light bars*) of simvastatin. (**f**) The CYP2D6 accessibility (*Ei*, *dark bars*) and probability function *PSMi* (*light bars*) of simvastatin.

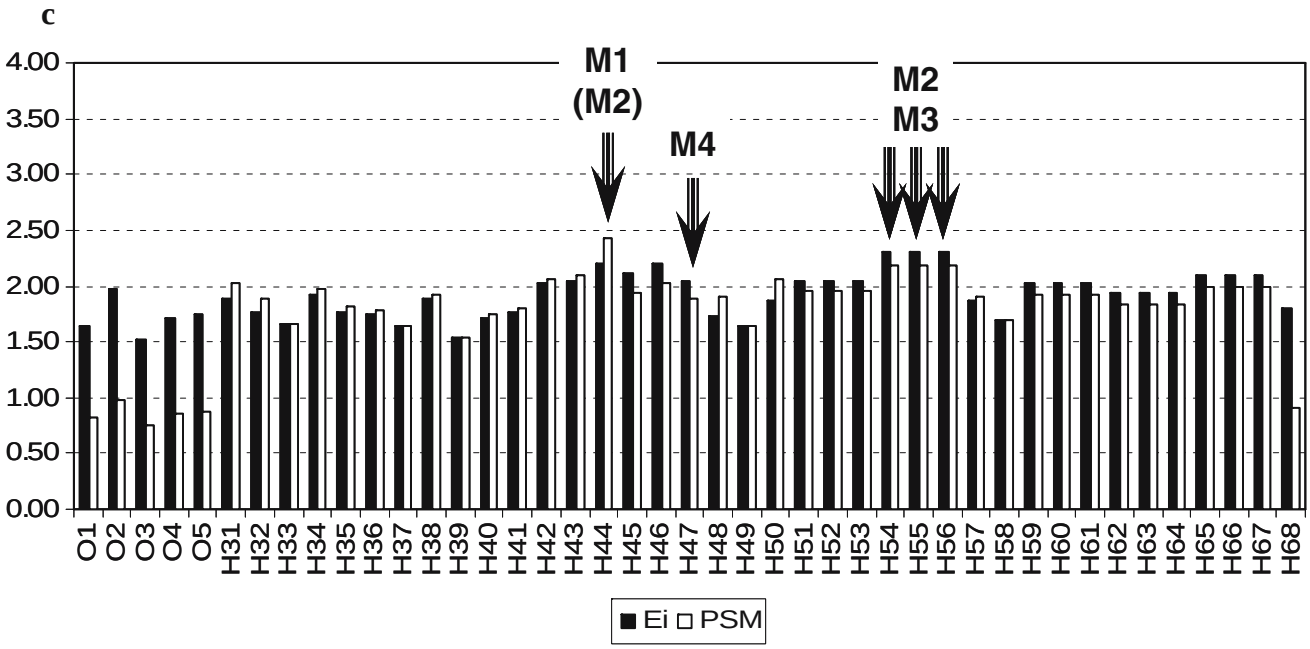

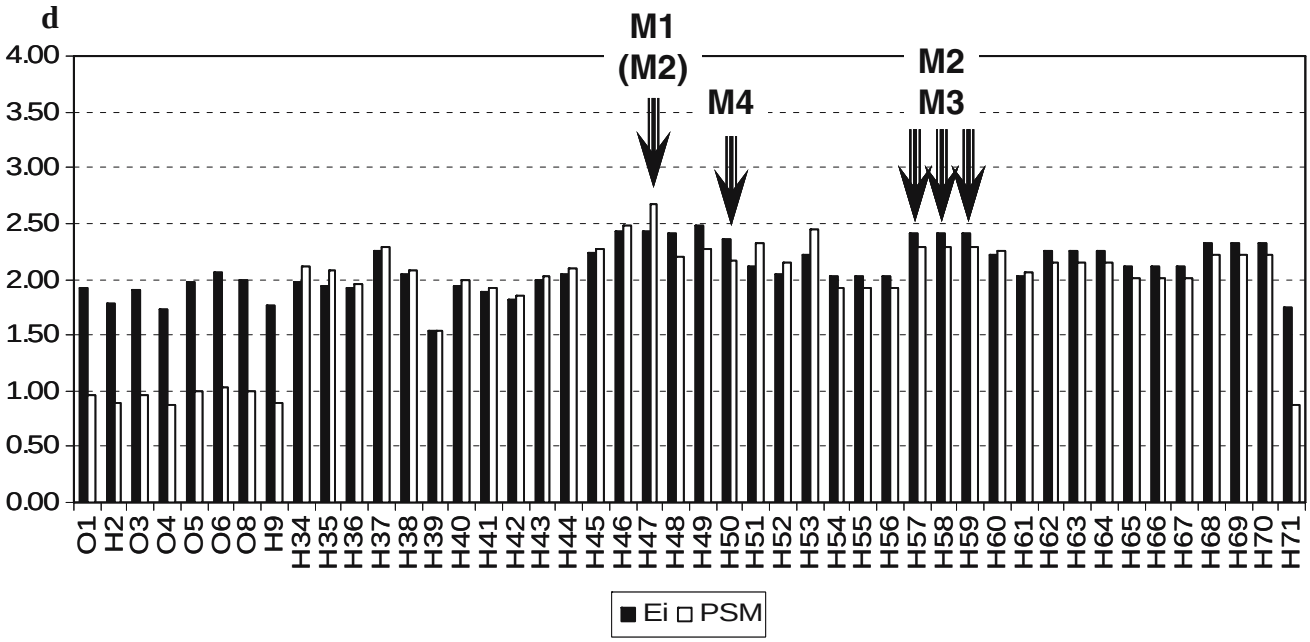

Fig. 7. (Continued).

C31 leads to metabolite *M1* which has the (*S*)-configuration at the newly created chiral center. This corresponds to the stereoselective abstraction of H59.

The second metabolite (*M2*) is an epoxide whose formation of was deduced from the structure of two stable metabolites, namely its glutathione conjugate and a product of non-enzymatic hydration and rearrangement (37,60).

The *MetaSite* models for CYP3A4 (Fig. 6c and d) and the other CYPs do indicate H59 (*M1* formation) as a probable site of attack (5th rank, Table I), but without preference over the geminal H58 (i.e., no stereoselectivity), and with a somewhat lower priority than some other sites such as C27 (H53, 1st rank, Table I) and C30 (H57, 3rd rank). As for the epoxide *M2* (epoxidation at C22-23), the H48 position receives a relatively low score (22nd rank) in the hydroxy-acid form, and a better one (7th rank) in the lactone (H46 position).

Simvastatin

Simvastatin, (1*S*,3*R*,7*S*,8*S*,8a*R*)-8-{2-((2*R*,4*R*)-4-hydroxy-6-oxo-3,4,5,6-tetrahydro-2*H*-pyran-2-yl)ethyl}-3,7-dimethyl-1,2,3,7,8,8a-hexahydronaphthalen-1-yl 2,2-dimethylbutanoate, is the lactone prodrug the corresponding hydroxy-acid form. Simvastatin (whose crystallographic structure is shown in Fig. 7a, (61) code EJEQAL in the Cambridge Database

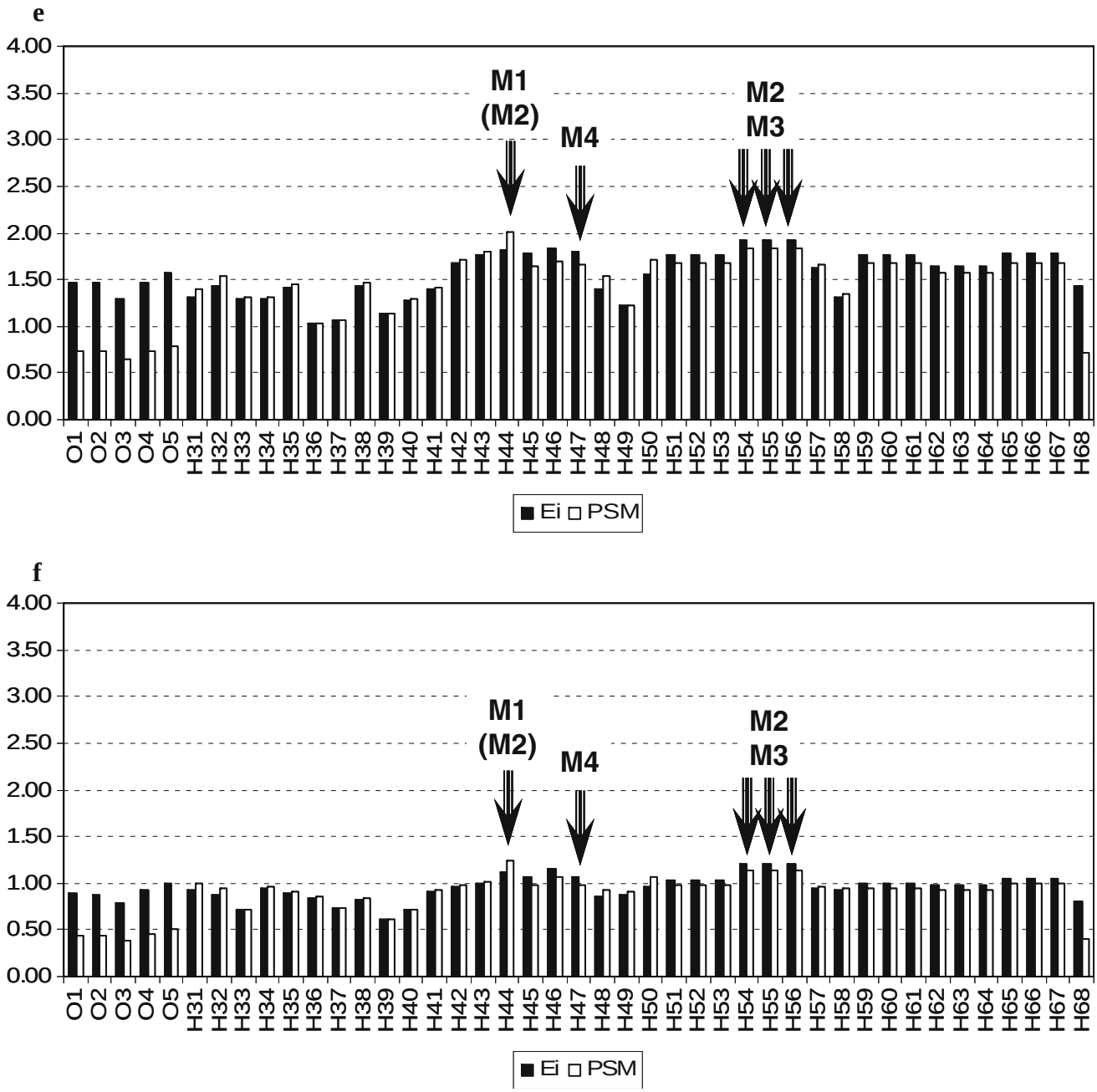

Fig. 7. (Continued).

(62)) is metabolized to at least four primary metabolites, namely 6′β-hydroxysimvastatin and the 6′-exomethylene metabolite (*M1* and *M2*, respectively) (Fig. 7b) (36,37). As for lovastatin, these two metabolites may well derive from a common metabolic precursor. A third product is the 6′β-hydroxymethyl metabolite (*M3*) which is further oxidized to 6′β-carboxysimvastatin, a metabolite excreted mostly via the bile in humans. A fourth metabolite is 3′-hydroxysimvastatin (*M4*) (63–65). CYP3A4 is the main human enzyme involved in the primary metabolism of simvastatin, although a moderate affinity for CYP2C9 and 2D6 has been documented, at least in the formation of *M2* and *M3*.

The primary site of CYP attack predicted by *MetaSite* for the lactone (Fig. 7c) is indeed at C15 (6′-hydroxylation by abstraction of H44, which leads to the important *M1* metabolite). As stated above, *M2* may also arise from the same initial attack, although it can also arise from hydroxylation at C24 (abstraction of H54 or H55 or H56) which is predicted to be second in importance. The same site yields *M3*, which is thus confirmed as a correct prediction. In contrast, attack at C19 (H47) to yield *M4* is not correctly predicted.

The CYP3A4 prediction for the hydroxy-acid form (Fig. 7d) was again correct for *M1*, bearing in mind that the abstracted hydrogen is renumbered H47. Here, formation of *M3* is no longer the second metabolite to be predicted.

Given the experimental finding that CYP2C9 and 2D6 also play a role in *M2* and *M3* formation, the corresponding *MetaSite* probability functions are shown for the lactone form

in Fig. 7e and f, respectively. The results for 2C9 (Fig. 7e) are in good agreement with experimental data, while the probability functions for 2D6 (Fig. 7f) are not sufficiently discriminative. The same is true for the probabilities histograms of CYP1A2 and 2C19 (results not shown), which are not known to oxidize simvastatin.

CONCLUSION

Statins undergo a multiplicity of metabolic pathways which result in a complex *in vivo* pattern of metabolites. Prediction of *in vivo* metabolic behavior will be based on accumulated knowledge obtained during *in vitro* investigations using increasingly complex biological tools (expressed enzymes, microsomes, cellular homogenates, cell cultures and *in situ* perfusions). *in silico* predictions of *in vivo* metabolites can also be of interest, but given the numerous metabolic pathways they involve, they need to rely on comprehensive experts systems such as rule-based algorithms (1,2,4,5).

In contrast, the early phases of drug discovery will focus mainly on *in vitro* assays using animal and human microsomes fortified with cofactors for cytochrome P450, given that approximately 80% of drugs are substrates of CYP-mediated redox attack during their phase I biotransformation. A predictive tool focusing on such early reactions is therefore an asset in drug discovery and may help drug designers and synthetic chemists obtain an estimate of the metabolically labile positions and of potential metabolites. Human experts can also benefit from such a system by comparing their predictions with those of the software and reasoning on differences. Another group of researchers able to benefit are the bioanalysts, who can for example deduce spectral characteristics from *in silico* predictions.

At the molecular level, the rate (and hence relative contribution) of a metabolic reaction is controlled by two factors, namely a productive binding to the enzyme involved (as assessed by Michaelis constant K_M), and the turnover of the catalytic reaction (as assessed by k_{cat} or V_{max}) in which the intrinsic reactivity of the target site plays a determining role. An attractive feature of *MetaSite* is its integration of these two factors, as quantified by the accessibility (recognition score, *Ei*) of atom *i* to the heme, and its chemical reactivity *Ri*. The comparison of the fingerprints of the binding/catalytic site with the fingerprints of the substrate allows the accessibility parameter to be calculated for each specific enzyme, whereas reactivity is parameterized based on a mixture of molecular orbital calculations and fragment recognition. Given the assumptions and simplifications implicit in these procedures, perfect predictions are neither expected nor claimed. This is particularly true for reactivity predictions, whose failure to account correctly for aromatic sites is evidenced in this work. This raises the question whether *MetaSite* should be preferred over docking strategies? The answer depends on the information one wishes to obtain, since docking reveals binding modes and even relative affinities, whereas *MetaSite* offers rapid predictions on the most probable sites of metabolic oxidation.

But the final lesson to be learned from studies such as this one is that many neutral validations should be made public before the real potential of a software can be evaluated, its limits better understood, and its shortcomings identified and improved. And above all, evaluations such as this one demonstrate that the usefulness of predictive softwares critically depends on human experts able to compare predictions and experimental data, interpret the similarities and differences, and deduce courses of action.

ACKNOWLEDGEMENTS

GC and GE are indebted to the University of Turin for financial support. The authors thank Silvia Tonelli for the preliminary work carried out during her undergraduate period of study. Molecular Discovery is also acknowledged for a free license and technical support.

Supporting Information Available: Corresponding atoms in the lactone and hydroxy-acid forms together with the complete lists of *PSMi*, E_i and R_i data for all investigated compounds.

REFERENCES

1. B. Testa and G. Cruciani. Structure–metabolism relations, and the challenge of predicting biotransformation. In B. Testa, H. van de Waterbeemd, G. Folkers, and R. H. Guy (eds.), *Pharmacokinetic Optimization in Drug Research: Biological, Physicochemical and Computational Chemistry*, Wiley-VHCA, Zurich, 2001, pp. 65–84.
2. B. Testa and W. Soine. Principles of drug metabolism. In D. J. Abraham (ed.), *Burger's Medicinal Chemistry and Drug Discovery*, Wiley-Interscience, Hoboken, N.J., USA, 2003, pp. 431–498.
3. P. W. Erhardt. *Metabolism Databases and High. Throughput Tesing During Drug Design and Development*, Blackwell Science, London, UK, 1999.
4. S. A. Kulkarni, J. Zhu, and B. S. Lechinger. *in silico* techniques for the study and prediction of xenobiotic metabolism: a review. *Xenobiotica* **35**:955–973 (2005).
5. B. Testa, A. L. Balmat, and A. Long. Predicting drug metabolism: concepts and challenges. *Pure Appl. Chem.* **76**:907–914 (2004).
6. B. Testa, A. L. Balmat, A. Long, and P. Judson. Predicting drug metabolism—an evaluation of the expert system METEOR. *Chem. Biodivers.* **2**:872–885 (2005).
7. B. Testa, P. Crivori, M. Reist, and P. A. Carrupt. The influence of lipophilicity on the pharmacokinetic behavior of drugs: concepts and examples. *Perspect. Drug Discov. Des.* **19**:179– 211 (2000).
8. C. Hansch, S. B. Mekapati, A. Kurup, and R. P. Verma. QSAR of Cytochrome P450. *Drug Metab. Rev.* **36**:105–156 (2004).
9. J. E. Penzotti, G. A. Landrum, and S. Putta. Building predictive ADMET models for early decisions in drug discovery. *Curr. Opin. Drug Discov. Dev.* **7**:49–61 (2004).
10. D. Korolev, K. V. Balakin, Y. Nikolsky, E. Kirilov, Y. A. Ivanenkov, N. P. Savchuk, A. A. Ivashchenko, and T. Nikolskaya. Modeling of human cytochrome P450-mediated durg metabolism using unsupervised machine learning approach. *J. Med. Chem.* **46**:3631–3643 (2003).
11. D. L. Harris. *In silico* predictive metabolism: a structural/electronic filter method. *Curr. Opin. Drug Discov. Dev.***7**:43–48 (2004).
12. J. P. Jones, M. Mysinger, and K. R. Korzekwa. Computational models for cytochrome P450: a predictive electronic model for aromatic oxidation and hydrogen atom abstraction. *Drug Metab. Dispos.* **30**:7–12 (2002).
13. R. N. Hines, Z. Luo, T. Cresteil, X. Ding, R. A. Prough, J. L. Fitzpatrick, S. L. Ripp, K. C. Falkner, N.-L. Ge, A. Levine, and

C. J. Elferink. Molecular regulation of genes encoding xenobiotic-metabolizing enzymes: mechanisms involving endogeneous factors. *Drug Metab. Dispos.* **29**:623–633 (2001).
14. M. D. Segall, M. C. Payne, S. W. Ellis, G. T. Tucker, and P. J. Eddershaw. First principles investigation of singly reduced cytochrome P450. *Xenobiotica* **29**:561–571 (1999).
15. P. A. Smith, M. J. Sorich, R. A. McKinnon, and J. O. Miners. Pharmacophore and quantitative structure–activity relationship modeling: complementary approaches for the rationalization and prediction of UDP-glucuronosyltransferase 1A4 substrate selectivity. *J. Med. Chem.* **46**:1617–1626 (2003).
16. S. Ekins, D. M. Stresser, and J. A. Williams. *In vitro* and pharmacophore insights into CYP3A enzymes. *TIPS* **24**:161–166 (2003).
17. A. Poso, J. Gynther, and R. Juvonen. A comparative molecular field analysis of cytochrome P450 2A5 and 2A6 inhibitors. *J. Comput.—Aided Mol. Des.* **15**:195–202 (2001).
18. L. Afzelius, I. Zamora, C. M. Misimirembwa, A. Karlén, T. B. Andersson, S. Mecucci, M. Baroni, and G. Cruciani. Conformer- and alignment-independent model for predicting structurally diverse competitive CYP2C9 inhibitors. *J. Med. Chem.* **47**:907–914 (2004).
19. I. Zamora, L. Afzelius, and G. Cruciani. Predicting drug metabolism: a site of metabolism prediction tool applied to the cytochrome P450 2C9. *J. Med. Chem.* **46**:2313–2324 (2003).
20. M. J. Sorich, J. O. Miners, R. A. McKinnon, and P. A. Smith. Multiple pharmacophores for the investigation of human UDP-glucuronosyltransferase isoform substare selectivity. *Mol. Pharmacol.* **65**:301–308 (2004).
21. J. Venhoorst, A. M. ter Laak, J. N. M. Commandeur, Y. Funae, T. Hiroi, and N. P. E. Vermeulen. Homology modeling of rat and human cytochrome P450 2D (CYP2D) isoforms and computational rationalization of experimental ligand-binding specificities. *J. Med. Chem.* **46**:74–86 (2003).
22. D. F. V. Lewis. Homology modelling of human CYP2 family enzymes based on the CYP2C5 crystal structure. *Xenobiotica* **32**:305–323 (2002).
23. D. F. V. Lewis. Molecular modeling of human cytochrome P450-substrate interactions. *Drug Metab. Rev.* **34**:55–67 (2002).
24. A. M. ter Laak and N. P. E. Vermeulen. Molecular modeling approaches to predict metabolism and toxicity. In B. Testa, H. van de Waterbeemd, G. Folkers, and R. H. Guy (eds.), *Pharmacokinetic Optimization in Drug Research*, Wiley-VCH, Zürich, 2001, pp. 551–588.
25. P. A. Williams, J. Cosme, A. Ward, H. C. Angove, D. Vinkovic, and H. Jhoti. Crystal structure of human cytochrome P450 2C9 with bound warfarin. *Nature* **424**:464–468 (2003).
26. P. A. Williams, J. Cosme, D. Vinkovic, A. Ward, H. C. Angove, P. J. Day, C. Vonrhein, I. J. Tickle, and H. Jhoti. Crystal structures of human cytochrome P450 3A4 bound to metyrapone and progesterone. *Science* **305**:683–686 (2004).
27. S. Ekins, E. Andreyev, A. Ryabov, E. Kirillov, E. A. Rakhmatulin, A. Bugrim, and T. Nikolskaya. Computational prediction of human drug metabolism. *Expert. Opin. Drug Metab. Toxicol.* **1**:303–324 (2005).
28. A. Endo. The origin of the statins. *Int. Congr. Ser.* **1262**:3–8 (2004).
29. T. Walley, P. Folino-Gall, U. Schwabe, and E. van Ganse. Variation and increase in use of statins across Europe: data from administrative databases. *Br. Med. J.* **328**:385–386 (2004).
30. B. Testa and J. M. Mayer. Hydrolysis in Drug and Prodrug Metabolism—Chemistry, Biochemistry and Enzymology, Wiley-VHCA, Zurich, 2003, pp. 493–495.
31. B. A. Hamelin and J. Turgeon. Hydrophilicity/lipophilicity: relevance for the pharmacology and clinical effects of HMG-CoA reductase inhibitors. *TIPS* **19**:26–37 (1998).
32. M. J. Kaufman. Rate and equilibrium constants for acid-catalyzed lactone hydrolysis of HMG-CoA reductase inhibitors. *Int. J. Pharm.* **66**:97–106 (1990).
33. D. E. Duggan, I.-W. Chen, W. F. Bayne, R. A. Halpin, C. A. Duncan, M. S. Schwartz, R. J. Stubbs, and S. Vickers. The physiological disposition of lovastatin. *Drug Metab. Dispos.* **17**:166–173 (1989).
34. H. Fujino, T. Saito, Y. Tsunenari, J. Kojima, and T. Sakaeda. Metabolic properties of the acid and lactone forms of HMC-CoA reductase inhibitors. *Xenobiotica* **34**:961–971 (2004).
35. T. Prueksaritanont, B. Ma, X. Fang, R. Subramanian, J. Yu, and J. H. Lin. β-oxidation of simvastatin in mouse liver preparations. *Drug Metab. Dispos.* **29**:1251–1255 (2001).
36. M. J. Garcia, R. F. Reinoso, A. Sanchez Navarrro, and J. R. Prous. Clinical pharmacokinetics of statins. *Meth. Fin. Exp. Clin. Pharmacol.* **25**:457–481 (2003).
37. U. Christians, W. Jacobsen, and L. C. Floren. Metabolism of drug interactions of 3-hydroxy-3-methylglutaryl coenzyme a reductase inhibitors in transplant patients: are the statins mechanistically similar?. *Pharmacol. Ther.* **80**:1–34 (1998).
38. D. Zhou, L. Afzelius, S. W. Grimm, T. B. Andersson, R. J. Zauhar, and I. Zamora. Comparison of methods for the prediction of the metabolic sites for CYP3A4-mediated metabolic reactios. *Drug Metab. Dispos.* **34**:976–983 (2006).
39. G. Cruciani, R. Vianello, and I. Zamora. Prediction of site of metabolism in humans: case studies of cytochromes P450 2C9, 2D6 and 3A4. In B. Testa, S. Kraemer, H. Wunderli-Allenspach, and G. Folkers (eds.), *Pharmacokinetic Profiling in Drug Research: Biological, Physicochemical and Computational Strategies*, Wiley-VHCA, Zürich, 2005, pp. 367–379.
40. G. Cruciani, E. Carosati, B. De Boeck, K. Ethirajulu, C. Mackie, T. Howe, and R. Vianello. MetaSite: understanding metabolism in human cytochromes from the perspective of the chemist. *J. Med. Chem.* **48**:6970–6979 (2005).
41. D. N. A. Boobbyer, P. J. Goodford, P. M. McWhinnie, and R. C. Wade. New hydrogen-bond potentials for use in determining energetically favorable binding sites on molecules of known structure. *J. Med. Chem.* **32**:1083–1094 (1989).
42. P. J. Goodford. A computational procedure for determining energetically favorable binding sites on biologically important macromolecules. *J. Med. Chem.* **28**:849–857 (1985).
43. R. C. Wade, K. J. Clark, and P. J. Goodford. Further development of hydrogen bond functions for use in determining energetically favorable binding sites on molecules of known structure. I. Ligand probe groups with the ability to form two hydrogen bonds. *J. Med. Chem.* **36**:140–147 (1993).
44. R. C. Wade and P. J. Goodford. Further development of hydrogen bond functions for use in determining energetically favorable binding sites on molecules of known structure. II. Ligand probe groups with the ability to form more than two hydrogen bonds. *J. Med. Chem.* **36**:148–156 (1993).
45. A. R. Leach, B. K. Shoichet, and C. E. Peishoff. Prediction of protein–ligand interactions. Docking and scoring: successes and gaps. *J. Med. Chem.* **49**:5851–5855 (2006).
46. MOE, version 2005.06, 2005,. Chemical Computing Group, Montreal, Quebec Canada, http://www.chemcomp.com/.
47. T. A. Halgren. MMFF VI. MMFF94s option for energy minimization studies. *J. Comput. Chem.* **20**:720–729 (1999).
48. Vega, version 2.0.5., 2006, http://www.ddl.unimi.it/.
49. G. Caron, G. Ermondi, A. Damiano, L. Novaroli, O. Tsinman, J. A. Ruell, and A. Avdeef. Ionization, lipophilicity, and molecular modeling to investigate permeability and other biological properties of amlodipine. *Bioorg. Med. Chem.***12**:6107–6118 (2004).
50. D. Qiu, P. S. Shenkin, F. P. Hollinger, and W. C. Still. The GB/SA continuum model for solvation. A fast analytical method for the calculation of approximate born radii. *J. Phys. Chem., A.* **101**:3005–3014 (1997).
51. T. Sakaeda, H. Fujino, C. Komoto, M. Kakumoto, J. Jin, K. Iwaki, K. Nishiguchi, T. Nakamura, N. Okamura, and K. Okumura. Effects of acid and lactone forms of eight HMG-CoA reductase inhibitors on CYP-mediated metabolism and MDR1-mediated transport. *Pharm. Res.* **23**:506–512 (2006).
52. W. F. Trager. Principles of drug metabolism 1: redox reactions. In B. Testa and H. van de Waterbeemd (eds.), *Comprehensive Medicinal Chemistry, 2nd Edition, Volume 5*, Elsevier, Oxford, UK, 2006, pp. 87–132.
53. M. Boberg, R. Angerbauer, P. Fey, W. K. Kanhai, W. Karl, A. Kern, J. Ploschke, and M. Radtke. Metabolism of cerivastatin by human liver microsomes *in vitro*. *Drug Metab. Dispos.* **25** 321–331 (1997).
54. T. Prueksaritanont, J. J. Zhao, B. Ma, B. A. Roadcap, C. Tang, Y. Qiu, L. Liu, J. H. Lin, P. G. Pearson, and T. A. Baillie. Mechanistic studies on metabolic interactions between gemfibrozil and statins. *J. Pharmacol. Exp. Ther.* **301**:1042–1051 (2002).
55. M. Boberg, R. Angerbauer, W. K. Kanhai, W. Karl, A. Kern, M.

Radtke, and W. Steinke. Biotransformation of cerivastatin in mice, rats, and dogs *in vivo*. *Drug Metab. Dispos.* **26**:640–652 (1998).
56. W. Jacobsen, G. Kirchner, K. Hallensleben, L. Mancinelli, M. Deters, I. Hackbarth, L. Z. Benet, K.-F. Sewing, and U. Christians. Comparison of cytochrome P-450-dependent metabolism and drug interactions of the 3-hydroxy-3-methylglutaryl-CoA-reductase inhibitors lovastatin and pravastatin in the liver. *Drug Metab. Dispos.* **27**:173–179 (1998).
57. B. Testa. *The Metabolism of Drugs and Other Xenobiotics—Biochemistry of Redox Reactions*, Academic, London, UK, 1995.
58. H. Fujino, I. Yamada, S. Shimada, M. Yoneda, and J. Kojima. Metabolic fate of pitavastatin, a new inhibitor of HMG-CoA reductase: human UDP-glucuronosyltansferase enzymes involved in lactonization. *Xenobiotica* **33**:27–41 (2003).
59. B. Testa and S. Kraemer. The biochemistry of drug metabolism. An introduction. Part 2. Redox reactions and their enzymes. *Chem. Biodivers.* (2007) (in press).
60. D. W. Everett, T. J. Chando, G. C. Didonato, S. M. Singhvi, H. Y. Pan, and S. H. Weinstein. Biotransformation of pravastatin sodium in humans. *Drug Metab. Dispos.* **19**:740–748 (1991).
61. J. Cejka, B. Kratochvil, I. Cisarova, and A. Jegorov. Simvastatin. *Acta Crystallogr.* **C59**:o428–o430 (2003).
62. F. H. Allen. The Cambridge structural database: a quarter of a million crystal structures and rising. *Acta Crystallogr.* **B58**:380–388 (2002).
63. R. Subramanian, X. Fang, and T. Prueksaritanont. Structural characterization of *in vivo* rat glutathione adducts and a hydroxylated metabolite of simvastatin hydroxy acid. *Drug Metab. Dispos.* **30**:225–230 (2006).
64. S. Vickers, C. A. Duncan, I.-W. Chen, A. Rosegay, and D. E. Duggan. Metabolic disposition studies of simvastatin, a cholesterol-lowering product. *Drug Metab. Dispos.* **18**:138–145 (1990).
65. S. Vickers and C. A. Duncan. *In vitro* and *in vivo* biotransformation of simvastatin, an inhibitor of HMG-CoA reductase. *Drug Metab. Dispos.* **18**:476–483 (1990).